SSRG International Journal of Civil Engineering
ISSN: 2348-8352/ https://doi.org/10.14445/23488352/IJCE-V13I4P116

Volume 13 Issue 4, 244-274, April 2026


*Original Article*

# Experimental Evaluation of Sustainable Thermal Roofing Using Plant Fibers and Activated Pineapple Charcoal to Mitigate the Impact of Frost on Homes in the High Andes

Jose Antonio Roque Cardenas[1], Joel Dalmacio Navarro Navarro[1], Abigail Cenith Mendoza Cabrera[1], Juan Elias Otarola Santivañez[1*]

[1]*Faculty of Architecture, Continental University, 12001, Huancayo, Perú.*

**Corresponding Author : jotarola@continental.edu.pe*

Received: 12 January 2026 Revised: 14 February 2026 Accepted: 18 March 2026 Published: 28 April 2026

***Abstract -*** *In the high Andean regions of Peru, frost causes extreme temperature drops that affect the health and comfort of rural populations, whose adobe homes lack insulation. The high transmittance of metal roofs and energy poverty increase vulnerability, requiring sustainable, low-cost solutions based on local materials. This research experimentally evaluated the thermal efficiency of adobe roofs modified with ichu, Linen, and activated pineapple shell charcoal in different proportions to determine the optimal doses for insulation and hygrothermal regulation. Ten 1:5 scale prototypes were built, one control and nine with adobe modified with ichu (30%, 33%, and 36%), Linen (57%, 60%, and 63%), and activated carbon (10%, 15%, and 20%). Each model replicated a rural dwelling with a corrugated iron roof sloping 13.5° to the south and 5 cm of adobe thermal mass to maximize heat capture. Temperature, relative humidity, and wind speed were monitored for 24 hours, at 15-minute intervals between 04:00 and 07:00 a.m., using calibrated digital instruments. The results showed notable thermal improvements compared to the exterior: ICHU at 33% maintained 9.5 °C, Linen at 60% reached 11.0 °C, and activated carbon at 20% reached 12.0 °C, with lower interior humidity. It is concluded that the incorporation of plant fibers and agro-industrial waste into adobe roofs offers a sustainable alternative for mitigating frost in rural high Andean dwellings.*

***Keywords -*** *Thermal roofs, Modified adobe, Plant fibers, Activated carbon, High Andean dwellings.*

## 1. Introduction

In Peru, adobe is a fundamental material in rural construction due to its low cost, local availability, and ancestral tradition [1]. According to the 2017 National Census, more than 2.1 million homes (27.9% of the total) still use adobe or rammed earth as a construction system [2]. In the Junín region, particularly in the province of Huancayo, the use of adobe remains predominant in rural and peri-urban areas, where nearly 46% of dwellings use compacted earth [3, 4]. Despite its high thermal inertia, adobe has limitations in terms of thermal comfort, particularly in high Andean areas, where night-time temperatures drop sharply [5]. Added to this are the poor thermal conditions of the dwellings, the absence of adequate heating systems, and energy poverty, factors that considerably increase the risks for the populations living in these regions [6]. In this context, frost is a critical climatic phenomenon in the high Andean areas of Peru, especially above 3,000 metres above sea level, where temperatures drop below 0°C during the night and early morning, directly affecting the rural population [7]. The impact on health is alarming, with children under five and older adults being the most vulnerable to the increase in acute respiratory diseases and pneumonia. In 2025, at least 45 deaths of people over 60 years of age from pneumonia were reported [8]. This problem is not unique to Peru. In the Bolivian highlands, where many families live in precarious adobe and thatched homes, temperatures dropped to -14°C, causing 23 deaths from hypothermia [9]. Recently, between June and July 2024, the department of La Paz recorded 16 deaths due to extreme cold, reflecting the persistent vulnerability to low temperatures in these regions [10]. In Nepal, during the winter of 2021, several deaths from hypothermia were recorded in the Tarai districts, where dozens of people from poor communities die every year due to extreme cold in adobe houses without insulation or adequate heating. Many victims died inside their homes while trying to keep warm with braziers in enclosed spaces, which also caused smoke poisoning, highlighting the vulnerability of these traditional dwellings to low temperatures [11]. As a result, various studies have shown that, in adobe houses without thermal insulation, indoor temperatures can be extremely low, creating conditions of severe discomfort [12, 13]. On the one hand, research has identified that poor insulation, especially in roofs, is a key factor in thermal discomfort in rural high Andean dwellings in Peru, where low-

cost improvements such as the use of expanded polystyrene in roofs, doors and floors, together with passive elements such as skylights and ceilings, have been proposed, achieving a notable improvement in interior comfort [14]. On the other hand, research has been conducted on incorporating natural additives into adobe to improve its thermal performance [15]. The study also incorporates the use of recycled peanut shells as a plant-based binding agent. Adding 7% to 9% peanut shells can reduce thermal conductivity by 50% without compromising structural strength. This makes the use of agricultural waste a viable option for rural construction [16]. This confirms the study where the incorporation of 4% cement with 1% plant fibers in adobe blocks was in the cement range that reduced thermal conductivity and improved mechanical performance [17]. However, despite these advances, existing studies have mainly examined individual additives or industrial insulation alternatives, without providing a comparative assessment of locally available natural materials under the same experimental conditions. In particular, there is limited evidence on the individual thermal performance of ichu fiber, flax fiber, and activated carbon derived from pineapple peel when each is separately incorporated into adobe mixtures for roofing applications in high-Andean environments. This lack of comparative and context-specific evidence constitutes a research gap, especially in Huancayo, where local materials may represent sustainable and low-cost alternatives for reducing thermal discomfort in rural housing. Therefore, this study addresses the problem of the low thermal performance of traditional adobe roofing in high-Andean dwellings exposed to frost by evaluating adobe modified with three materials available in the Huancayo region to determine their effectiveness as building materials capable of improving thermal behaviour under severe climatic conditions. The first additive is ichu, which has been experimentally shown to have favourable thermal and mechanical behaviour, achieving a 28% reduction in thermal conductivity compared to typical adobe, while meeting structural strength and interior comfort standards [18]. The second additive is flax fiber, which has been shown to improve the insulating quality of earthen compounds due to its low thermal conductivity and high heat retention [19]. The third additive is activated carbon from pineapple peels, a scarcely studied material in adobe-based construction, known for its high porosity and efficient adsorption properties, making it promising for functional thermal improvement and environmental regulation in building materials [20]. In Huancayo, pineapple peel waste is produced in abundance and is currently discarded, along with other organic waste, in local markets, juice bars, and fruit shops. This case is a great example of how this waste can be recycled and reused as a sustainable input for new, improved (adobe-based) building materials [21].

The novelty of this research lies in the experimental comparison of three locally available and sustainable additives, namely ichu fiber, flax fiber, and activated carbon from pineapple peel, each incorporated individually into adobe mixtures under identical conditions. This approach allows the specific thermal contribution of each material to be identified in frost-prone high-Andean environments, using resources that are readily available in Huancayo. Although some analyses have been completed recently, little is known about the impact of individual proportions of ichu fiber, flax fiber, and activated carbon from pineapple peel on the thermal properties of adobe mixtures. Accordingly, this study aims to experimentally evaluate the effect of different dosages of each additive on the thermal behaviour of sustainable adobe roofing mixtures, in order to identify the most effective material for improving thermal comfort in high-Andean rural housing. Therefore, the research seeks to generate technical evidence for the selection of optimal low-cost and locally available materials for improving thermal comfort in rural housing.

## 2. State of the Art

### *2.1. Adobe and Natural Fibers for Thermal Improvement in High-Andean Housing*

Several studies have investigated the incorporation of natural fibers into adobe and earthen materials to improve their thermal performance in cold climates. Among these, researchers from the Faculty of Sciences at the National University of Engineering conducted an assessment of the impact of ichu fiber on the thermal and mechanical behaviour of adobe mixtures in Lima. Using local soil with 33% ichu by volume, blocks were made and subjected to thermal conductivity (ASTM C177) and compressive strength (E.080) tests. With a thermal conductivity of 0.349 W/m·K and a compressive strength of 2.41 N/mm², sufficient for adobe (0.371 W/m·K), a 5.9% reduction was recorded compared to adobe. The study concludes that ichu is a valuable improvement over adobe in the Andean rural housing model [22]. Similarly, at the Pontifical Catholic University of Peru, an experimental study has been completed with the same objectives of evaluating the thermal behaviour of ichu conglomerates to establish their use as insulation in dry construction systems in high Andean regions. To this end, panels were made with ichu fibers in two formats: flat panel and conglomerate, testing thicknesses of 5 cm, 10 cm, and 20 cm. Thermal conductivity was evaluated using the transient hot plate method, and the thermal transmittance (U) of a system composed of fiber cement + insulation + fiber cement was calculated. The results showed that the 10 cm thick conglomerate panels achieved an average thermal conductivity value of 0.0943 W/m·K, and wall systems with this insulation achieved a thermal transmittance of 0.419 W/m²K, complying with the limit values established by the RNE for cold climates. In addition, the study concluded that ichu is highly available, low-cost, and has a low environmental impact, positioning it as an efficient, ecological, and economically viable alternative for improving thermal comfort in rural homes in high Andean areas [23].

In Arequipa, researchers from the Academic Department of Physics at the University of San Agustin de Arequipa and

the Faculty of Sciences at the National University of Engineering developed an experimental Guarded Hot Plate Apparatus (GHPA) system with Peltier cell cooling to evaluate the thermal conductivity of insulating materials typical of high Andean regions, such as adobe with ichu, ashlar, glass, and sugarcane bagasse. Double circular samples were placed on both sides of a circular hot plate, with cold plates at the ends cooled by liquid. The measurement was performed under controlled conditions, with one-dimensional heat flow and E and K-type sensors. The proportions of the materials were not detailed except in the case of adobe, to which approximately 10% Stipa ichu fiber was added. The results showed low thermal conductivity values, with sugarcane bagasse being the most efficient (0.04 W/m·°C), followed by adobe with ichu (0.20 W/m·°C), ashlar (0.29 W/m·°C), and finally glass (0.65 W/m· °C). The system required between 3 and 7 hours to reach thermal equilibrium in each case. The study concluded that the proposed GHPA system is accurate and efficient for the thermal characterisation of materials, and that the materials evaluated, due to their low cost and local availability, are suitable for use in homes in high Andean areas vulnerable to cold [24]. On the other hand, researchers from the Academic Department of Physics at the University of San Agustin De Arequipa developed a low-cost portable system to measure the thermal conductivity of materials used in buildings in high Andean areas, with the aim of evaluating traditional materials in situ as thermally efficient alternatives. A unidirectional heat flow model was used through 4.0 cm × 4.2 cm × 1.35 cm samples, heated by screen-printed resistors and cooled by a cold plate system with Peltier cells. Four materials were analysed: glass, ignimbrite (ash), roof tiles, and adobe with Stipa ichu fiber. The latter was manufactured with an estimated proportion of 10% ichu, achieving a thermal conductivity of 0.34 W/m·°C, slightly lower than that of brick (0.58 W/m·°C) and better than that of glass (0.97 W/m·°C). The measurements were taken after thermal equilibrium was reached, with test times of 2.5 to 5.5 hours and temperature gradients between 19.4 and 39.1 °C. The results confirmed that Adobe with ichu has competitive thermal performance and that the proposed system allows materials to be evaluated directly in a rural context. It is concluded that the equipment built is effective and accurate, and that traditional materials such as adobe and ignimbrite remain more thermally appropriate than conventional options such as brick or concrete [25].

In Lima, researchers from the University of Engineering and Technology conducted a study focused on characterising the thermal properties of ichu fiber (Stipa ichu) as a low-cost natural insulator, with the aim of improving thermal conditions in rural high Andean dwellings. Samples of fine and coarse ichu, with average diameters of 0.39 mm and 0.83 mm, respectively, obtained in the province of Canchis (Cusco), were evaluated using a Guarded Hot Plate system designed in accordance with ASTM C177. The tests were carried out with fibers arranged in unidirectional and non-unidirectional (random) mats, as well as configurations with crushed and uncrushed fibers. In the unidirectional configuration, the lowest thermal conductivity was obtained with uncrushed fine ichu: 0.0473 W/m·K (density: 92.86 kg/m³), comparable to commercial glass fibers (0.0355 W/m·K). By randomly rearranging the fibers, a significant reduction in density was achieved without a critical increase in thermal conductivity. SEM analyses revealed hexagonal porous structures in stems and leaves, responsible for the low thermal conductivity. The study concludes that ichu fiber, especially fine and non-oriented fiber, has great potential as a natural, economical thermal insulator applicable to roofs and walls of homes in cold rural areas [26].

Overall, the reviewed studies consistently demonstrate that ichu is a locally available, low-cost, and thermally efficient material with considerable potential for improving the performance of adobe and other earthen systems in high-Andean environments. However, most previous investigations have focused either on the intrinsic thermal properties of ichu, its use in insulation panels, or its incorporation into adobe at a single proportion. Consequently, there is still limited comparative evidence regarding its thermal behavior under different dosages within roofing applications subjected to frost conditions.

### *2.2. Thermal Potential of Flax/Linen-Based Materials*

Flax and linen-based materials have gained increasing attention as sustainable thermal insulators due to their low density, low thermal conductivity, renewable origin, and potential for valorizing agricultural residues. In this context, an experimental study conducted in Egypt investigated the use of linen fiber waste for the manufacture of thermal insulation panels for buildings as an alternative to conventional insulating materials. Twenty-five panel samples were produced, varying the proportion of two types of Linen waste (residual Linen fibre and Linen “machine tow”), the type of binder (natural gum arabic, polyester and AOS foaming agent), thickness (2.5 to 40 mm), density (0.025 to 0.65 g/cm³), and reinforcement layers such as aluminium foil and air bubbles.

The most common fiber-to-binder ratio was 60:40, and some samples were enriched with 6% paraffin. Thermal conductivity was measured using a modified hot box chamber. The most notable results show that the most efficient panel (sample 24), composed of Linen waste, paraffin, an aluminium foil, and a layer of air bubbles (7.5 mm thick), achieved a thermal conductivity of 0.0298 W/m·K m·K, outperforming commercial materials such as mineral wool, polystyrene foam (EPS/XPS), and fiberglass. The conclusion indicates that Linen waste can be transformed into high-performance, environmentally friendly, and cost-effective thermal panels with properties comparable to and even superior to traditional insulation, provided that their manufacturing and composition variables are optimised [27].

In the United Kingdom, the environmental performance of eleven bio-based insulation materials, including Linen, was assessed using a life cycle analysis based on scenarios combined with a dynamic assessment. Data from literature and databases such as ecoinvent were used to model each material in terms of manufacturing, transport, and end of life, considering a reference period of 60 years. For Linen, reference thermal properties with a conductivity of 0.038 W/m·K and an average density of 23 kg/m³ were used, although variations between 20 and 80 kg/m³ were analysed. The results revealed that, although Linen has relatively high manufacturing impacts due to the use of fertilisers and plastic additives, its overall impact (GWP100) remained below that of other conventional materials, such as Polyurethane (PUR). In addition, the dynamic assessment showed that plant-based materials, including Linen, have the potential to temporarily store carbon, helping to mitigate climate change in the short term. However, this benefit depends on proper recycling at the end of its useful life. In conclusion, Linen proved to be a viable option as bio-based thermal insulation, with competitive environmental impacts and adequate technical properties, although its sustainability is significantly improved when responsible agricultural practices and efficient manufacturing processes are implemented [28].

In Lithuania, the thermal behaviour of natural Linen fibres processed using different mechanical methods was evaluated in order to determine their potential as an ecological insulator. The study used Linen stems harvested in the north of the country, which were subjected to roller scutching, cutting, and chopping processes at different lengths (2-3 cm and 5-7 cm), obtaining combed and chopped fibers. The prepared samples, with densities between 39.6 and 102.5 kg/m³, were analysed according to EN 12667 and EN 12939 standards using Fox-304 equipment at 10 °C. The results indicated that the thermal conductivity of Linen fibers varied between 0.0341 and 0.0432 W/m·K for combed fibers of 2 to 3 cm, showing that density and processing method significantly influence insulation. It was concluded that short fibers processed with rollers represent an optimal, economical, and sustainable option for the manufacture of bio-based insulation materials, provided that the microstructure and cleanliness of the input material are adequately controlled [29].

In China, researchers investigated the use of residual Linen fiber after the Linenseed harvest, obtained at the Inner Mongolia Academy of Agricultural Sciences. To do this, fibrous bundles were extracted manually, subjected to alkaline treatments with NaOH (10 and 20 g/L), and used as reinforcement in Poly(Butylene Succinate) (PBS) composites manufactured by thermal compression. The main input was the post-linseed Linen fiber bundle, with a composition of 40.11% cellulose, 28.27% hemicellulose, and 15.08% lignin, which is significantly different from textile Linen. The mechanical properties of the bundles and composites were evaluated: the tensile strength of the untreated bundle was 1.14 cN/dTex, and that of the PBS/fiber composite was 78.2 MPa (untreated), improving flexural strength to 49.16 MPa with alkaline treatment. SEM analysis showed that surface treatment improves fibre-matrix adhesion. The results demonstrate that post-linseed Linen fiber, whether treated or untreated, is suitable for technical applications and industrial composites, contributing to the valorisation of an underutilized agricultural waste product [30].

In France, researchers investigated the production and properties of Linen fiber from oilseed crops (seed Linen) in the south-western region of the country, using the Everest variety. The study used stems collected after the Linenseed harvest, which were subjected to different pre-treatments of soaking and re-moistening, and processed in a Laroche Cadette 1000 industrial machine to separate the plant fractions on a pilot scale. Parameters such as fiber yield, length, diameter, and tensile strength of the fibers obtained were measured. The results showed that the extraction allowed between 38% and 40% of the dry weight of the stem to be recovered as fiber, with average lengths of 3.7 to 5.3 cm, diameters of 20 to 23 μm, and average tensile strength of 324 to 377 MPa, reaching maximum values of up to 980 MPa. These figures demonstrated that post-linseed Linen fiber, although slightly inferior in properties to textile Linen, is suitable for technical applications such as reinforcement in composites or geotextiles, and that its use represents an economically attractive and sustainable alternative for oilseed Linen agricultural waste [31].

### *2.3. Activated Carbon and Porous Materials for Thermal Regulation*

Porous and high-surface-area materials have been increasingly investigated for their potential to regulate heat transfer, improve thermal storage, and modify the physical performance of construction materials. In this context, although not focused directly on thermal insulation, a study conducted in Italy examined the use of reactive fine additives to improve the performance of vulnerable adobe bricks. The researchers proposed a consolidation treatment based on the activation of Ground Granulated Blast-Furnace Slag (GGBS) with calcium hydroxide nanoparticles, aiming to form hydrated calcium silicate gel in situ as a compatible binder within the adobe matrix. Four formulations were prepared using different concentrations of $Ca(OH)_2$ and GGBS, with and without ethanol as a dispersing medium. Among them, the formulation based on nano-$Ca(OH)_2$ in water exhibited the highest efficiency, producing a greater amount of C-S-H in a shorter time. When applied to adobe blocks from Morelos, Mexico, and cured for 28 days, the treatment reduced total porosity from 10% to 5%, doubled the abrasion coefficient from 130 to 247 cm²/g, and decreased the surface decohesion index from 0.75 to 0.37 mg/cm². Confocal Raman spectroscopy, SEM, and microtomography confirmed the formation and penetration of C-S-H within the pore structure.

Although this study was oriented toward mechanical consolidation rather than thermal insulation, it demonstrated that fine and reactive porous modifiers can substantially alter the internal structure and performance of adobe-based materials [32].

More directly related to thermal regulation, a research team in South Korea investigated the incorporation of activated carbon into underfloor heating systems in combination with paraffin as a thermal storage material. The study addressed known limitations of phase change materials, particularly low thermal conductivity and phase leakage under varying temperature conditions. To overcome these issues, the researchers prepared a stable composite material through vacuum impregnation of paraffin wax into porous activated carbon and placed it inside PVC containers for heating-system applications. The results showed that the addition of activated carbon increased thermal conductivity to values close to 2.5 W/m·K, which was up to 3.81 times higher than that of pure PCM. In addition, the material retained 66.18% of its mass after the first stage of thermal decomposition, although this occurred with a reduction of 60.7% in latent heat storage capacity. When integrated into underfloor systems together with linoleum, the activated carbon–paraffin composite reduced surface temperature deviation to 1.7 °C, thereby improving thermal stability and indoor comfort. These findings confirmed that activated carbon can play an important role as a thermal stabilizer and heat-transfer enhancer in building-related applications [33].

### *2.4. Research Gap and Novelty of the Present Study*

Recent research has demonstrated the growing potential of sustainable materials such as ichu, flax, and activated carbon for improving thermal performance, mechanical behaviour, and energy efficiency in construction and related fields. Due to their low cost, local availability, and environmentally friendly nature, these materials have been widely explored in applications such as insulation panels, passive heating systems, and environmental remediation processes. However, most of these studies have been developed in isolated or highly specific contexts, without integrating these materials into conventional construction systems such as adobe. In particular, existing research shows that ichu is the only material among those studied that has been experimentally incorporated into adobe mixtures, mainly at specific dosages and under limited conditions. In contrast, the incorporation of flax fibers into adobe has been scarcely documented, and there is currently no evidence of the use of activated carbon as an additive in adobe-based materials. Furthermore, previous investigations have generally evaluated these materials independently, making it difficult to establish direct comparisons of their thermal performance under equivalent experimental conditions. This limitation is especially relevant in high-Andean regions, where roofing systems play a critical role in heat loss and thermal discomfort during frost periods.

In this context, the novelty of the present study is based on the experimental evaluation and comparison of three sustainable additives: ichu fiber, flax fiber, and activated carbon obtained from pineapple peel, each one incorporated individually into adobe roofing systems under the same conditions. Through the analysis of different dosages and the monitoring of thermal behaviour using temperature and environmental variables, this research offers new comparative evidence. In this way, it contributes to the identification of low-cost, locally available materials that can be used to improve thermal comfort in rural housing located in high-Andean areas.

## 3. Materials and Methods

This section details the materials used in the production of modified adobe and the experimental procedures used for the preparation and characterisation of ichu fibers, flax fibers, and activated carbon from pineapple peels. It describes the steps involved in collecting and conditioning materials and incorporating them into adobe mixtures, as well as the techniques and conditions used to evaluate the thermal and mechanical behaviour of the samples.

### *3.1. Adobe*

Adobe, a traditional building material, is composed of earth and water, which is then moulded into blocks and dried in the sun, completely omitting the firing process [34, 35]. Although the building material is cheap and accessible, especially in rural areas, it has many disadvantages in construction. The limitations of the material include a lack of compressive and tensile strength, fragility, a lack of moisture resistance, and high maintenance requirements. These disadvantages have led to the incorporation of reinforcement strategies, including the use of natural fibers and other stabilisers that improve the thermal and mechanical performance of the materials [36, 37].

The properties of the building material are summarised in Table 1, where thermal conductivity, 0.799 W/(m·K), stands out as a key characteristic that determines the insulating properties of the material. Lower thermal conductivity improves heat retention, increases comfort, and reduces the energy use of the materials. Building material imports are also optimised by using natural fiber additives, resulting in efficient and sustainable building materials. The optimised building material is particularly suitable for construction in cold climates.

**Table 1. Properties of Adobe [37]**

| Property | Value |
|---|---|
| Compressive strength | 4.80 MPa |
| Dry density (ρ) | 1935 kg/m³ |
| Porosity | 36.5 % |
| Moisture content | 2.0 % |
| $CaCO_3$ content | 84.9 % |
| Thermal conductivity (λ) | 0.799 W/(m·K) |

According to Table 1, the physical and thermal characteristics of adobe demonstrate the importance of complying with all processing stages in accordance with Peruvian Technical Standard E.080, Design and Construction with Reinforced Earth. This standard helps to achieve structural and thermal durability, reliability, and overall performance of the heat retention capabilities of the materials used, thus contributing to the comfort and sustainability of the building over the years [34].

*3.1.1. Obtaining Adobe*

The production and preparation of adobe complied with Peruvian Technical Standard E.080, as shown in Figure 1. Part a) illustrates the material extraction stage, indicating that the soil was collected by hand at the Uñas quarry in the Huancayo region (coordinates 12°01'55.0‘S 75°11'18.0’W). The extraction was carried out at a depth of approximately 50 cm to avoid the surface layer rich in organic matter, obtaining a clayey soil (SC) with a high proportion of fines (41.61% passes through sieve No. 200), which favoured its cohesion and plasticity (Plasticity Index PI = 18.79%) [38]. Subsequently, as shown in item b, the collected material was sieved and stored using a #4 mesh (4.75 mm) to remove stones, plant debris, and large clods, ensuring a homogeneous soil texture. Finally, the screened material was placed in clean buckets for storage until it was mixed with the additives (ichu, Linen, and activated carbon) in the previously determined proportions.


**Fig. 1 Soil selection procedure for adobe**

***3.2. Prototype***

After reviewing technical standards, regulations, and national and international scientific literature, it was found that there were no provisions defining the size of prototypes in experimental studies on adobe housing. Peruvian Technical Standard E.080 ‘Adobe’ does not establish minimum or maximum dimensions for interior spaces, as its focus is on structural safety [34].

*3.2.1. Size of Adobe Dwellings*

In the absence of specific regulations, a review was conducted to identify the conventional dimensions of adobe dwellings in rural areas of Peru, taking as a reference those that faithfully represented traditional construction practices, and then scaling them according to their use. When analysing the size of the dwellings reported in more than 1,000 cases documented by aid programs, university studies, and field surveys, it was observed that the usable areas ranged from 12 to 56 m², with walls approximately 2.4 m high and 40 cm thick, and adobe blocks measuring approximately 40 × 40 × 10 cm. This dimensional convergence, despite regional and methodological diversity, made it possible to establish a representative range for prototype design [39]. Therefore, a 25 m² (5 m × 5 m) model was adopted as a reference, with a rear height of 3.20 m and a front height of 2 m, compatible with the common dimensions observed and suitable for scale replication.

*3.2.2. Prototype Scale*

For the development of the prototype, previous research on small-scale housing construction, mainly 1:1 and 1:5, was reviewed, especially that related to architectural validation, spatial functionality, thermal comfort, and rural applications [1, 40]. It is in this context that a scale of 1:5 was chosen, as this scale seemed to offer adequate geometric construction detail and reliability for evaluating thermal comfort [41-43]. The prototype was based on a real house model with a footprint of 5 m × 5 m, a rear height of 3.20 m, and a front height of 2.00 m. When scaled, the house model was 1 m × 1 m, with heights of 0.64 m at the rear and 0.40 m at the front, and replicated the characteristics of a single-pitched roof. This configuration maintained the original geometry and proportions and therefore ensured that the prototype presented optimal conditions for thermal analysis while thermally representing the original house model. Furthermore, the principles of heat and moisture transfer remain unchanged in all scaled models, and therefore, the results can be fully extrapolated to the scale models as long as the geometric proportions and materials are maintained [44].

*3.2.3. Roofing Material*

In the high Andes of Peru, the most common type of roofing material used in homes is corrugated iron, which accounts for 34.9% of urban housing and 58.1% of rural housing. Although widely used, it has thermal deficiencies due to its high transmittance and susceptibility to cold air penetration, leading to thermal discomfort in cold climates. However, some previous studies have indicated positive attributes such as a strong structure, adequate performance in extreme environments, rapid daily heat gain and loss, and resistance to freeze-thaw cycles, which support its selection for high Andean environments [14, 45]. Therefore, in this study, considering the extensive literature and high frequency of such materials in rural construction, corrugated iron was selected as the roofing material for the prototype and was useful for evaluating thermal performance under real conditions [46, 47]. The orientation and slope of the roof directly influence the thermal behaviour of homes, especially in cold areas. Research has shown that the best thermal configuration for metal roofs in cold climates is a 15° south-

facing slope, which recorded the highest interior temperature (Vti = 30.9 °C) due to its high solar exposure during the day and its ability to promote heat accumulation [48, 49]. Based on this evidence, a single-slope metal roof with a 13.5° slope facing south was chosen, not only as a passive strategy to maximise solar radiation capture during the day and facilitate thermal accumulation in the modified adobe volume, but also to standardise measurements and optimise the execution of the full-scale prototype.

*3.2.4. Placement of Improved Adobe under the Roof*

Thermal efficiency in passive roofs is significantly increased when the thermal mass is located directly under the roof covering, without intermediate air chambers [50]. Several studies have shown that this proximity favours heat capture and transfer. They emphasised that placing the storage material directly under the roof improves heat gain and subsequent release, recommending distances of 0 to 2 cm and thicknesses of 10 to 25 cm to achieve efficient storage [51, 52]. For this reason, in the present prototype, it was decided to use a distance of 0 cm, placing the modified adobe thermal mass directly under the metal roof, in order to optimise heat accumulation and release in high Andean conditions. Figure 2 shows the construction details of this configuration, including the specifications adopted for the location and thickness of the thermal mass under the roof.

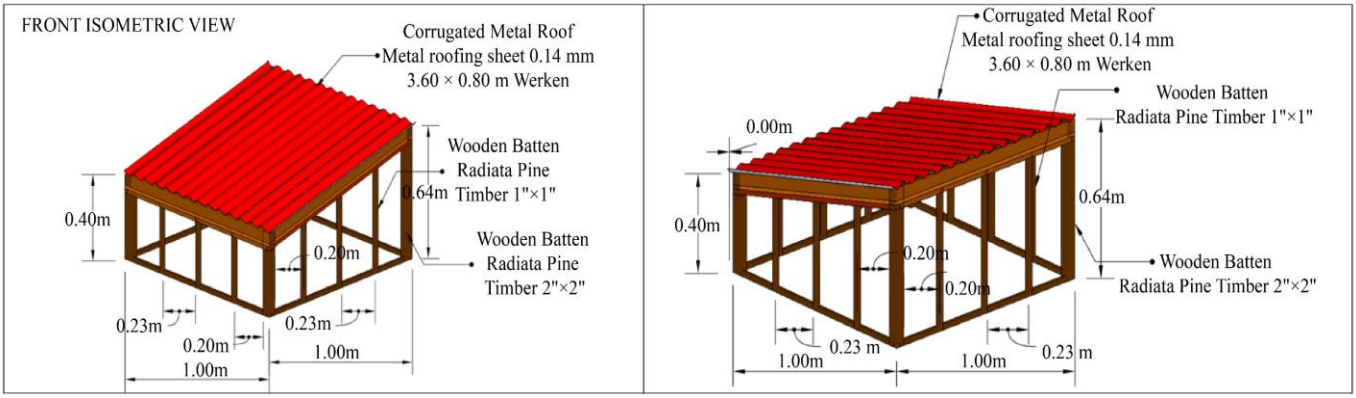


**Fig. 2 Prototype model**

Non-structural adobe blocks measuring 0.25 × 0.25 m and 5 cm in thickness were used as thermal mass in the prototype roof. This configuration was selected to maximise the amount of heat-accumulating material per unit area, thereby improving thermal inertia and contributing to the stabilisation of day-night temperature fluctuations in cold climates. The blocks were positioned directly on a ¾" square galvanised mesh that offered full support. Because of its direct contact with the adobe, the mesh quickly achieved thermal equilibrium with the blocks, enabling uniform heat transfer that maximised the system's performance as a passive insulating layer.

*3.2.5. Support Beams, Columns, and Prototype Walls*

A cross-section of wooden beams of 1" × 1" was chosen for its lightweight and ease of installation. 40.618 kg/m was analysed and is shown in Figure 6 as a total distributed load, which includes only the weight of the corrugated iron and the adobe slab. This configuration was adopted considering that the structure will not be subjected to dynamic or residential loads, but exclusively to controlled conditions for measuring the temperature in the interior environment, as shown in Figure 3.

Wooden columns differentiated according to their location were used for the structure. At the ends, 2" x 2" (4.1 cm x 4.1 cm) sections were used, as these dimensions facilitated the execution of firm joints using 2" long nails with a diameter of 2.4 mm. Although the structural analysis indicated that the columns would only be subjected to an axial load well below the permissible capacity of 1920.8 kgf, which would have allowed the use of 1" x 1" sections, it was preferred to maintain the 2" x 2" sections for construction and safety reasons. On the other hand, in the side columns, where multiple joints were not required, and the stresses were lower, 1" x 1" sections were chosen to optimise the use of materials without compromising the stability of the system. These details are shown in Figure 4.

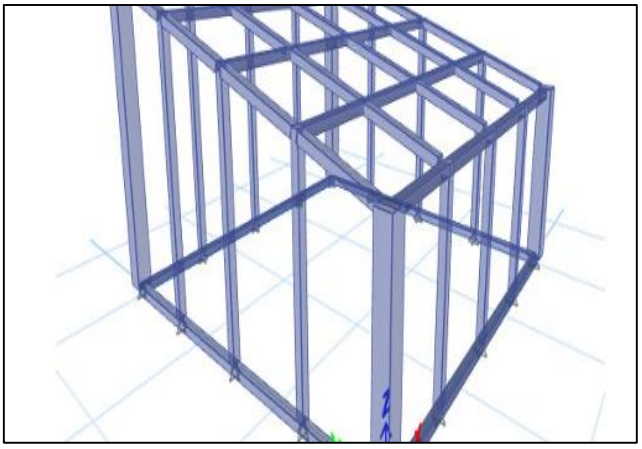

**Fig. 3 Mathematical model**

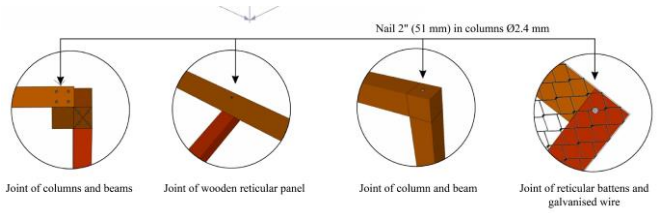


**Fig. 4 Details of element joints**

Finally, for the prototype walls, the criterion of experimental simplification applied in the research carried out in the community of Aramachay was taken into consideration, where phenolic plywood was used to facilitate the installation of sensors and control thermal conditions during testing [53]. Therefore, in order to assimilate the thermal behaviour of adobe without physically replicating it, fiber cement (4 mm Volcanboard) was used as the enclosure material. This choice was based on its ease of construction, dimensional stability, and, especially, its thermal conductivity comparable to that of adobe [54], which allows for adequate representation of heat transmission through the walls. By avoiding the complications arising from moisture, cracking, and the heterogeneity of raw adobe, it was ensured that the thermal measurements obtained accurately reflected the effect of the insulation system.

*3.2.6. Prototype Assembly*

The prototype was built following a carefully controlled procedure to ensure both dimensional accuracy and structural stability (Figure 5). Initially (item a), the wooden elements of the main frame were cut according to the design specifications using precision power tools, with joint angles systematically checked. The components were then assembled using 2″ galvanised nails to form the base frame, providing the required rigidity (item b). Subsequently (item c), fiber-cement panels were installed on the side and rear walls and fixed with self-tapping screws, allowing the structure to remain stable while representing the intended thermal enclosure. In item d, a ¾″ square galvanised mesh was placed over the frame to serve as continuous support for the adobe block mass. The structure was then positioned according to the design criteria (item e), defining a south-facing roof slope of 13.5° to maximise solar exposure and thermal performance. Finally, the corrugated metal sheets were cut and fitted to the roof geometry (item f), completing the full assembly of the prototype (item g), which was then ready for the incorporation of the improved adobe mixtures while preserving the intended geometry and representativeness of the construction.

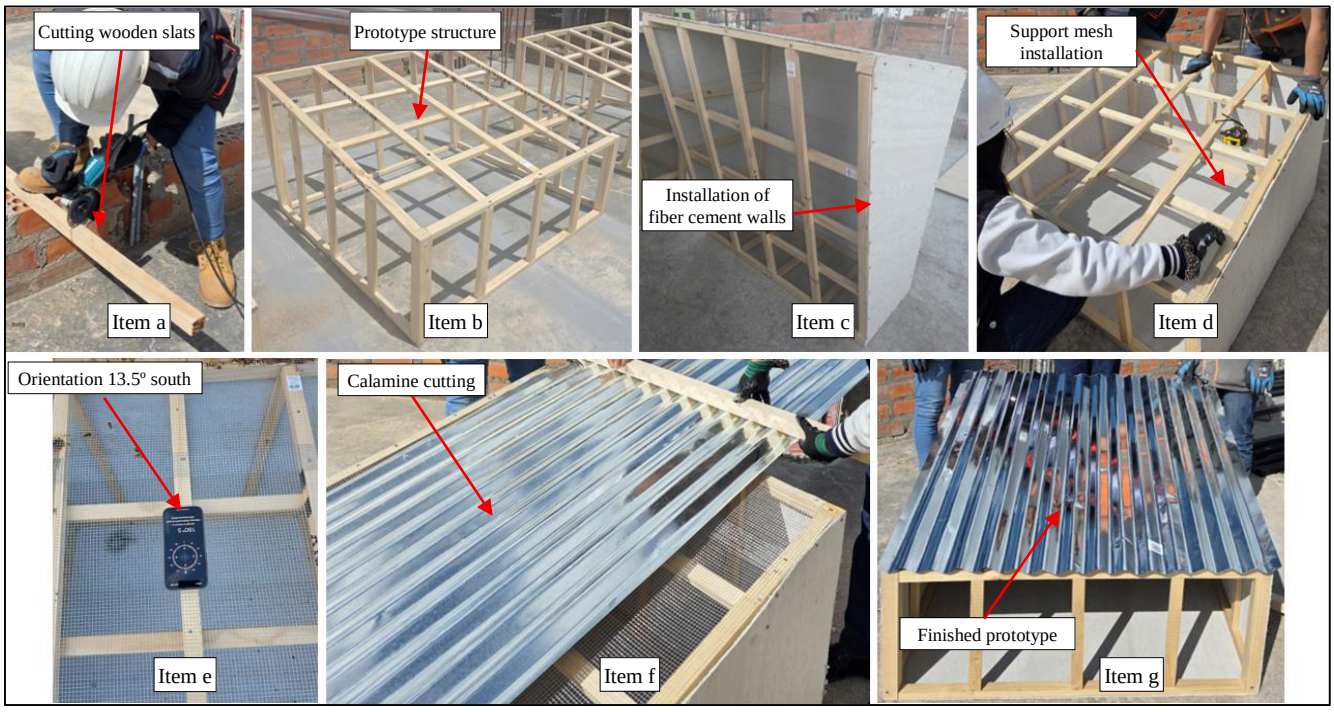


**Fig. 5 Prototype assembly**

*3.2.7. Heat Flow in the Prototype*

The experiment design considered the intensity of solar radiation and the location of the metallised roofing. Metallised roofing absorbs the radiation and conducts the heat to the blocks in the middle of the roofing. The blocks have high thermal mass and contact the roofing to absorb the heat and elevate the temperature of the blocks. The galvanised mesh retains thermal equilibrium with the adobe and does not obstruct the heat transfer. Therefore, the roofing acted as a thermal solar collector and the adobe mass trapped it, preventing transfer to the interior, which remained cool due to the thermal mass. The metal roofing loses heat and cools when

the sun sets; however, the adobe keeps the heat due to high thermal inertia. The system explains the reverse of thermal radiation as the metal roofing heats up the indoor space. Since the blocks were not insulated on the underside and were in direct contact with the internal air, they gradually released heat through radiation and convection, which allowed a more stable interior temperature to be maintained during the night. As a result, the thermal mass acted as a passive thermal regulator that delayed heat gain during the day and mitigated heat loss at night, contributing to thermal comfort without the need for active air conditioning systems. This process is illustrated in Figure 6.

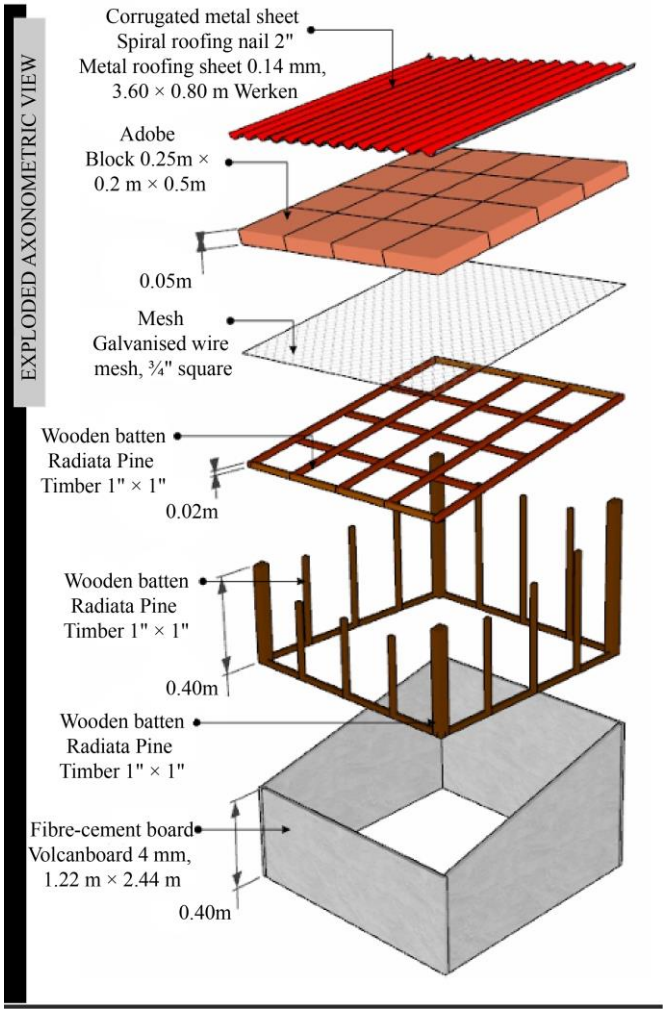


**Fig. 6 Details of element joints**

### *3.3. Ichu*

Soil Ichu is an Andean grass represented by the species Stipa obtusa and Jarava ichu, traditionally used in roofs and ropes, and currently evaluated as a natural fiber for composite materials [55]. It is a plant endemic to Peru that grows wild, with high availability (76,000 tonnes per year) and low harvesting costs (0.15 USD/kg) [56]. The main physical, chemical, and durability properties of ichu are summarised in Table 2.

**Table 2. Properties of Stipa Ichu [57]**

| Property | Description |
|---|---|
| **Scientific name** | Stipa ichu |
| **Common name** | Ichu, paja brava |
| **Growing altitude** | 3700 to 4800 m.s.n.m. |
| **Chemical composition** | 45.9% cellulose, 18.2% lignin, 5.5% pentosans, 5.6% ash |
| **Physical structure** | Tubular fiber, average diameter: fine (0.39 mm) / coarse (0.83 mm) |
| **Density** | 88.44 kg/m³ |
| **Porosity** | 58.29% |
| **Moisture content** | 11.21% |
| **Raw fibre** | 35.4% |
| **Fungal durability** | High resistance is classified as very durable. |
| **Thermal conductivity** | 0.037 W/m·K, ideal as thermal insulation. |
| **Fire resistance** | Good performance, charring slowly without rapid flame spread |
| **Sound absorption** | Reduces noise by 12 dB according to sound level meter tests |

Table 2 summarises the properties of ichu, highlighting in particular its low thermal conductivity (0.037 W/m·K) and high porosity (58.29%), characteristics that make it an excellent material for thermal insulation in adobe mixtures. Its low density and fibrous structure help reduce heat flow through the material, while its resistance to moisture and durability against fungi ensure good performance in the demanding conditions of the Andean climate. In the literature review, various proportions of ichu fiber incorporation in adobe mixtures were identified, among which the use of fine, uncrushed ichu in a proportion of 33% by volume with respect to the soil stood out [22]. This configuration allowed for a slight reduction in thermal conductivity and compliance with the compressive strength parameters established by Peruvian regulations [34]. Based on these results, the present research proposed the application of ichu fiber in proportions of 30%, 33%, and 36%. This progressive variation responds to the need to fill gaps in previous studies, which are often based on a single percentage and do not explore the influence of different dosages [22, 53]. Thus, the aim is to identify more precisely the optimal range for incorporating ichu that maximises the thermal performance of adobe without compromising its mechanical integrity. The following section describes in detail the procedure followed for obtaining and preparing the ichu fiber, as well as its incorporation into the experimental mixtures.

#### *3.3.1. Obtaining Ichu*

The procedure followed for obtaining and preparing Stipa ichu fiber was carried out in accordance with the guidelines

established in Peruvian Technical Standard E.080 [34, 38] This procedure is shown in Figure 7. Item a) shows the collection of plant material, where ichu, the predominant species in the high Andean grasslands of Huancayo, was obtained directly from the rural community of Saño, selecting thin, intact stems without physical alterations [58]. Subsequently, as shown in item b, the material was cleaned and dried under controlled environmental conditions at 18 °C, spreading it out on clean surfaces for 48 hours and avoiding direct exposure to the sun to preserve its flexibility and strength [59]. Drying lasted for 48 hours, avoiding direct exposure to sunlight in order to preserve the physical properties of the fiber and prevent it from becoming brittle. In item c, the fibers were cut manually to a length of 2.5 cm, ensuring their adequate dispersion in the soil mass. Then, in item d, the preparation of the base soil and the incorporation of ichu can be seen, carried out by manual mixing to ensure the uniform distribution of the fibers in proportions of 30%, 33%, and 36% with respect to the volume of dry soil. Finally, as shown in item e, the mixture was moulded manually in adobe formwork, applying pressure and slight vibrations to compact the material and reduce voids, leaving it to cure in the air for seven days in a ventilated environment protected from direct sunlight, in order to obtain homogeneous units, free of cracks and with progressive natural drying.

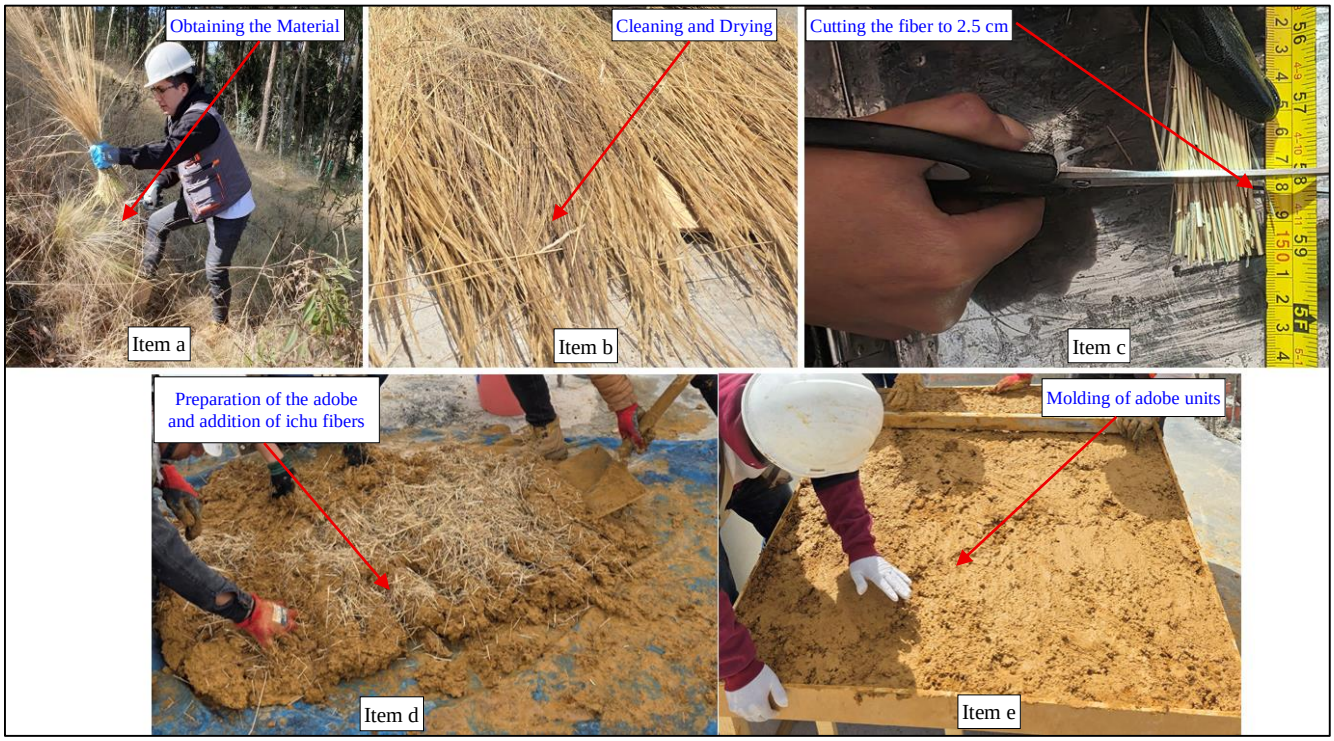


**Fig. 7 Soil selection procedure for adobe with Ichu**

### *3.4. Linen*

Linen is a natural plant fiber extracted from the stem of the Linum usitatissimum plant, widely valued for its renewable origin and low environmental impact. In addition to its mechanical qualities, this fiber stands out for its vibration-damping and sound insulation properties, characteristics that promote thermal and environmental comfort [60-62]. Table 3 describes the properties of Linen. Linen residue after the Linenseed harvest was used to produce materials for thermal comfort in construction, specifically as insulation. Although post-linseed Linen fiber had inferior mechanical properties compared to textile Linen, its structure and composition allowed its outstanding thermal and acoustic insulation qualities to be exploited, which was essential in applications where the main function was to reduce heat transfer and improve indoor comfort [29-31].

**Table 3. Properties of post-harvest Linen [29-31]**

| Property | Description |
|---|---|
| **Chemical composition (%)** | Cellulose: 40.11%, Hemicellulose: 28.27%, Lignin: 15.08%, Pectin: 6.3%, and Wax: 3.1% |
| **Individual tensile strength** | 324 MPa, |
| **Fibre diameter** | 20 μm |
| **Technical fiber length** | 3.7 cm |
| **Extracted fiber yield** | 40% |
| **Thermal conductivity** | 0.432 ·K |

#### *3.4.1. Obtaining Linen*

The procedure followed for obtaining and preparing the Linen fibre used in the adobe mixture was carried out in accordance with the guidelines of Peruvian Technical

Standard E.080 [34] and is illustrated in Figure 8. Item a shows the post-harvest collection of Linen stalks, carried out manually at the end of the mechanised harvest, using agricultural pitchforks and protective gloves. The stalks were grouped into bundles of 30 units and transferred to a covered and ventilated area, avoiding direct exposure to rain. Item b shows the initial drying process, where the bundles were placed on a clean plastic sheet, outdoors and in the shade for seven days, rotating them daily to ensure even drying until they became stiff and easy to break. Next, as shown in item c, the dry stems were chopped into 3 cm fragments using an electric chopper and then beaten with a wooden mallet to facilitate the manual release of the fibers, separating them from the shives. In item d, the extracted fibers were cleaned by manual shaking, using a fine-mesh metal sieve (2 mm) with repeated movements for 10 minutes per kilogram, in order to remove woody debris and surface dust. The fibers were then cut to a final length of 2.5 cm, grouped into bundles and short fragments discarded to ensure dimensional uniformity and ease of mixing. Finally, as shown in item f, the Linen fibres were gradually incorporated into the clay mixture, distributing them manually to achieve a homogeneous dispersion. From this point on, the procedure continued in a similar manner to that described for ichu in Figure 2, including the moulding of the adobe units and their natural curing for seven days, adapting the conditions of the process to the particular properties of Linen as a fibrous reinforcement.


**Fig. 8 Soil selection procedure for adobe with Linen**

### *3.5. Activated Carbon (AC)*

Activated carbon is a fine black powder obtained by intensely heating coal or other natural products, which generates a structure with a large number of microscopic pores [63]. This porosity allows it to trap and retain substances such as gases, liquids, and particles. Given its high level of porosity, activated carbon also has the potential to influence the thermal properties of materials [64]. Pineapple peel has proven to be a viable material for the production of activated carbon, mainly due to its high availability as an agricultural waste product generated in large volumes. The raw material was obtained from the Mercado Modelo de Huancayo, where the sale of pineapples generates a considerable amount of discarded peel every day. The use of activated carbon from pineapple peel not only contributes to the recovery of agro-industrial waste but also promotes the development of more sustainable environmental remediation technologies [65, 66]. The properties of activated carbon based on pineapple peel are presented in Table 4.

**Table 4. Properties of activated carbon from pineapple peel [67]**

| Property | Description |
|---|---|
| **Raw material** | Pineapple peel (agricultural waste) |
| **Activation method** | Activation with $ZnCl_2$ and carbonisation at 800 °C for 1 hour |
| **Structural property** | Porous and rough surface with cavities |
| **Thermal property** | High heat resistance due to high-temperature carbonisation, which improves the stability of the material. |
| **Functional groups (FTIR)** | Presence of OH and CH, which decrease after chemical activation |

| | |
|---|---|
| **Effective dose of adsorbent** | 4 grams to achieve maximum efficiency |
| **Main advantage** | Low cost, sustainable, and allows reuse of agro-industrial waste. |

Due to the properties detailed in Table 4, activated carbon obtained from pineapple peel through chemical activation and carbonisation has high potential for use as a thermal insulator in environmental comfort applications. The high porosity and highly developed surface structure, confirmed by Scanning Electron Microscopy (SEM), allow excellent air retention in the pores, which reduces heat transfer by conduction. In addition, the presence of functional groups such as hydroxyls and aliphatic chains on the surface, evidenced by FTIR spectroscopy, facilitates interaction with other materials, enabling its integration with Phase Change Compounds (PCMs) or polymer matrices to improve storage efficiency and thermal management [67]. In one study, activated carbon was used as a total replacement for coarse aggregate in proportions ranging from 243 kg/m³, depending on the mix design, representing approximately 15% by weight of the total dry materials in the mix [68]. As a result, between 10%, 15%, and 20% by weight of activated pineapple husk charcoal will be used as aggregate in adobe to improve its strength, thermal insulation, and durability, following experimental evidence in lightweight cementitious materials. This initiative outlines its scope as examining the potential of passive thermal insulation enhancement without compromising the integrity of the material.

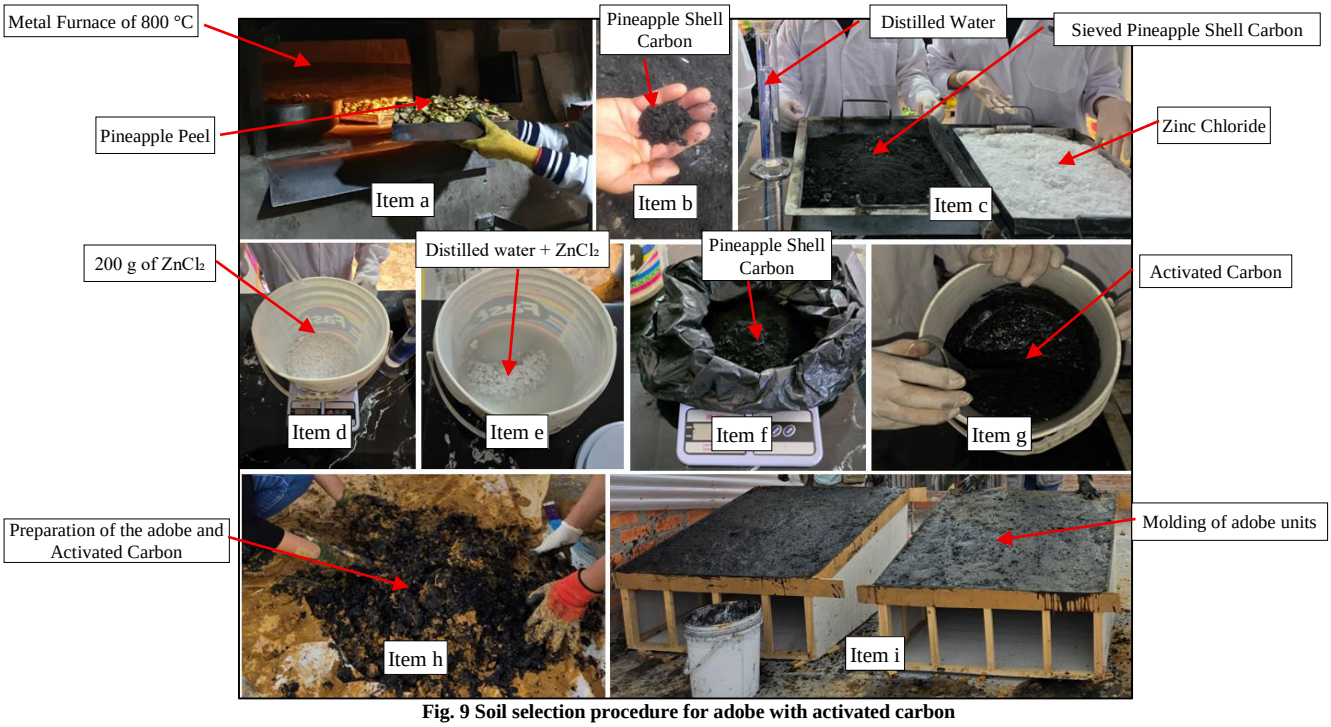


**Fig. 9 Soil selection procedure for adobe with activated carbon**

*3.5.1. Obtaining Activated Carbon from Pineapple Peel*

The procedure for obtaining and incorporating activated carbon from pineapple peel into the adobe mixture was developed in accordance with technical principles and scientific evidence [67], as shown in Figure 9. Item a) shows the collection and thermal carbonisation of pineapple peels, which were obtained fresh and clean from the Mercado Modelo de Huancayo, selecting those without mould or fermentation. They were then placed directly in a metal oven at a temperature of 800 °C for one hour, under partially closed conditions to control oxygen intake. In accordance with (item b), the cooled material was manually crushed to obtain a fine, homogeneous powder with a black colour and a porous structure suitable for chemical activation. Sieving of the resultant material was done with a No. 40 mesh (0.425 mm), removing coarse particles and retaining only the fine fraction for the impregnation process. The two input materials used for activation are listed in item c, these being dried, crushed carbon and solid zinc chloride ($ZnCl_2$), which serves as the activating agent. For item d, with the aid of a top balance, 200 g of $ZnCl_2$ was measured out and added to a beaker containing 1 liter of distilled water, and fully dissolved (item e) in order to prepare a homogeneous 20. Wt. % activating solution, which was prepared and kept at room temperature (18 °C). In item f, the dry carbon was fully submerged in the $ZnCl_2$ solution, and the system was left undisturbed for a duration of 24 hours to enable the activating agent to penetrate the pore structure of the dry carbon so as to increase the surface area of the dry carbon. The result of the activation process is shown in item g as a pasty, glossy black material with high apparent

density, which corresponds to activated carbon and is ready for use. Lastly (item h), the activated carbon was incorporated into the clay soil mixture in increments of 10%, 15%, and 20%. Furthermore, each increment was manually mixed until a uniform dispersion was visually achieved, ensuring that the carbon was integrated with the adobe matrix. Finally, as shown in item i, the mixture was moulded into adobe units and left to cure in the open air for seven days, in a ventilated environment protected from direct sunlight, allowing for progressive and uniform drying, without surface cracks and with adequate adhesion of the activated carbon within the structure of the material.

### *3.6. Thermal Comfort Measurement Indicators*

This research analysed temperature, humidity, and wind speed, as these are the most decisive indicators in assessing thermal comfort in high Andean dwellings, where extreme climatic conditions seriously compromise the habitability and health of their occupants [53].

#### *3.6.1. Data Collection*

Data was collected every hour during a complete 24-hour cycle, a methodology that allows for the capture of the most representative thermal variations in the environment [53, 69]. Likewise, this study incorporates a complementary strategy by establishing a higher measurement frequency every 15 minutes during the coldest hours of the day [70], between 4:00 and 7:00 a.m., according to official SENAMHI reports for the study area [71, 72]. This approach allows for a more accurate analysis of thermal conditions at times of greatest climatic vulnerability, when thermal comfort in high Andean dwellings is most compromised. In this way, the aim is for the results obtained to accurately reflect the effectiveness of the natural materials incorporated into adobe and to provide useful evidence for the design of construction solutions that improve the habitability of rural homes exposed to extreme cold.

#### *3.6.2. Temperature*

The ambient temperature corresponds to the air surrounding a material or system under normal conditions, without the direct influence of artificial heating sources [73]. A digital thermometer shown in Figure 10 was used for measurement. This instrument is essential in studies of thermal comfort and energy efficiency in buildings, as it allows accurate recording of ambient temperature in both indoor and outdoor spaces. Its use is essential in research on the thermal behaviour of homes and building materials, where reliable data is required to evaluate the performance of different architectural solutions and validate energy models [53, 74]. For this evaluation, the purpose of the measuring equipment was to be within the biothermal panels in order to collect data on the retention of heat within the rural dwellings. The insulation effect was direct, reflecting the internal microclimate and reducing the impact from the external conditions.


**Fig. 10 Thermometer - Hygrometer instrument**

#### *3.6.3. Humidity*

Within the prototype, moisture was measured using a digital hygrometer, which is shown in Figure 10. The quantification of the data is important because the relative humidity is a significant contributor to thermal comfort due to its impact on the body's ability to lose heat [75, 76]. Indoor measurements were important because of the prototype's design, which emphasizes the importance of indoor humidity and its impact on the risk of condensation and the evaluation of the internal climate's stability against the external climate's variability. The data was vital in evaluating the hygrothermal interrelation of the building materials and the indoor environment.

#### *3.6.4. Wind Speed*

Air speed was evaluated using a portable digital anemometer (Figure 11) to determine the extent of airflow and its effect on thermal comfort 77, 78]. Measurement was taken on the prototype's wind side, as wind is the only factor that can increase or decrease the heat gain and loss. The instrument enabled real-time recording of wind speed variations, providing reliable data for analysing its role in heat transfer.


**Fig. 11 Anemometer instrument**

## 4. Results

This section presents the results obtained from monitoring temperature, relative humidity, and wind speed in the experimental prototype. Measurements were taken systematically for each of the proposed additions of ichu, Linen, and activated pineapple husk charcoal, as well as for

the condition without additives. The aim is to demonstrate the effect of each material on the thermal performance of the roofing system, analysing the variations recorded during a complete 24-hour cycle and at critical times of minimum temperature, in order to determine the contribution of each addition to improving indoor thermal comfort.

### *4.1. Condition without Thermal Insulation*

Table 5 shows the thermal behaviour of the prototype without the addition of insulating materials during three consecutive days of monitoring. On day 1, the interior temperature of the prototype without additions behaved similarly to the outside environment, with slight differences due to the inertia of the confined air. The maximum external temperature was 29.3 °C at 1:00 p.m., while the internal temperature reached 28.7 °C, showing that solar heat was transmitted almost without attenuation through the metal roof. In the early morning, the interior temperature dropped to 13.8 °C at 5:30 a.m., practically equal to the exterior value (13.8 °C), indicating an absence of thermal retention. This behaviour is attributed to the high thermal conductivity and low thermal mass of the calamine, which enable rapid heat absorption during the day and accelerated heat loss at night. The indoor relative humidity increased progressively from dusk, reaching its maximum value of 44% Rh at 5:45 a.m., while the outdoor relative humidity was 43% Rh. This behaviour is a consequence of the calamine's high thermal conductivity and low thermal mass, which enables the formation of heat sinks by losing heat quickly at night after absorbing heat during the day. The lack of porous materials prevented this moisture from being absorbed, creating a more humid microclimate inside during the coldest hours. On day 2, the maximum outside temperature was 35.9 °C at 11:00 a.m., and the inside temperature was 33.5 °C, repeating the trend of direct solar heat transmission. In the early morning, the indoor temperature was 9.7 °C at 4:30 a.m., with an outdoor value of 9.6 °C, which again confirmed the thermal equalisation between indoors and outdoors. The indoor humidity reached 59% RH, slightly higher than the outdoor humidity (58% RH), due to the same effect of surface condensation and poor ventilation. Finally, on Day 3, the maximum outdoor temperature was 31.3 °C at 10:00 a.m., while the indoor temperature reached 30 °C, showing a slight reduction in daytime heat transfer. During the coldest hours, the indoor temperature dropped to 9.2 °C at 5:00 a.m., almost equal to the outdoor value (9 °C), showing that the roof without additions did not store thermal energy. Relative humidity ranged from 33% to 57% RH, practically similar to the ambient humidity, confirming the lack of hygrothermal control of the base system. Overall, the table showed that the roof without additions did not provide thermal or hygrometric buffering, with indoor temperatures and humidity levels almost equal to those outdoors. The unprocessed iron sheets acted as direct transmitters of climate change, without any thermal storage or regulation ability.

**Table 5. Condition without thermal insulation**

| Day | Day 1 | | | | | Day 2 | | | | | Day 3 | | | | |
|---|---|---|---|---|---|---|---|---|---|---|---|---|---|---|---|
| **Time** | **Out.** Temp. (°C) | **No add.** Temp. (°C) | **Out.** Hum. (%) | **No add.** Hum. (%) | **Out.** Wind (m/s) | **Out.** Temp. (°C) | **No add.** Temp. (°C) | **Out.** Hum. (%) | **No add.** Hum. (%) | **Out.** Wind (m/s) | **Out.** Temp. (°C) | **No add.** Temp. (°C) | **Out.** Hum. (%) | **No add.** Hum. (%) | **Out.** Wind (m/s) |
| **8:00 AM** | 18.4 | 18.3 | 43 | 44 | 0 | 28.2 | 28 | 38 | 40 | 0 | 20.8 | 20.7 | 42 | 43 | 0.1 |
| **9:00 AM** | 18.8 | 18.7 | 42 | 43 | 0 | 20.7 | 20.8 | 38 | 39 | 0 | 30.1 | 29 | 40 | 41 | 0.2 |
| **10:00 AM** | 21.7 | 21.4 | 41 | 42 | 0 | 19.9 | 20 | 38 | 40 | 0.1 | 31.3 | 30 | 33 | 34 | 0.6 |
| **11:00 AM** | 22.9 | 22.6 | 39 | 40 | 0 | 35.9 | 33.5 | 35 | 37 | 2.2 | 22.8 | 22.4 | 32 | 33 | 0.3 |
| **12:00 PM** | 24.4 | 24.1 | 38 | 39 | 0 | 22.5 | 22.1 | 37 | 38 | 0.2 | 24.2 | 23.8 | 33 | 34 | 0 |
| **1:00 PM** | 29.3 | 28.7 | 34 | 35 | 0 | 21 | 21.1 | 37 | 39 | 5.3 | 25.3 | 25 | 34 | 35 | 0 |
| **2:00 PM** | 24.2 | 23.9 | 34 | 35 | 0 | 19.5 | 19.8 | 37 | 38 | 1.1 | 24.5 | 24.2 | 34 | 35 | 0.3 |
| **3:00 PM** | 25.5 | 25.1 | 33 | 34 | 0.2 | 16.9 | 17.4 | 37 | 39 | 1.6 | 22.9 | 22.6 | 32 | 33 | 0.5 |
| **4:00 PM** | 23.3 | 23 | 34 | 35 | 0.3 | 15.3 | 15.5 | 45 | 47 | 0.8 | 22.3 | 22 | 33 | 34 | 0.6 |
| **5:00 PM** | 22.6 | 22.3 | 34 | 35 | 0.2 | 15.4 | 15 | 47 | 49 | 0.3 | 20.6 | 20.4 | 33 | 34 | 0.6 |
| **6:00 PM** | 21.4 | 21.2 | 35 | 36 | 0 | 14.6 | 14.3 | 48 | 50 | 0.6 | 19.6 | 19.5 | 35 | 36 | 0 |

| | | | | | | | | | | | | | | | |
|---|---|---|---|---|---|---|---|---|---|---|---|---|---|---|---|
| **7:00 PM** | 19.4 | 19.3 | 35 | 36 | 0 | 15.3 | 15.2 | 49 | 51 | 0 | 18.7 | 18.6 | 36 | 37 | 0 |
| **8:00 PM** | 18 | 17.9 | 37 | 38 | 0 | 15.9 | 15.7 | 49 | 50 | 0 | 18.4 | 18.3 | 35 | 36 | 0.1 |
| **9:00 PM** | 22.3 | 22 | 38 | 39 | 0 | 15.9 | 15.9 | 49 | 51 | 0.1 | 18.1 | 18 | 35 | 36 | 0 |
| **10:00 PM** | 20.9 | 21 | 38 | 39 | 0 | 17.3 | 17.1 | 50 | 52 | 0 | 17.7 | 17.7 | 34 | 35 | 0 |
| **11:00 PM** | 18.7 | 18.8 | 38 | 39 | 0 | 16.8 | 16.7 | 47 | 49 | 0.3 | 12 | 12.1 | 44 | 45 | 0 |
| **12:00 AM** | 18.9 | 19 | 39 | 40 | 0 | 16.6 | 16.3 | 47 | 48 | 0 | 12 | 12.1 | 49 | 50 | 0 |
| **1:00 AM** | 18.8 | 18.9 | 39 | 40 | 0 | 15.2 | 15.3 | 45 | 46 | 0 | 10.7 | 10.9 | 52 | 53 | 0 |
| **2:00 AM** | 18 | 18.1 | 40 | 41 | 0 | 15.2 | 15.1 | 49 | 50 | 0.1 | 9.9 | 10 | 53 | 54 | 0 |
| **3:00 AM** | 17.8 | 17.9 | 41 | 42 | 0 | 13.6 | 13.4 | 48 | 49 | 0.3 | 9.5 | 9.7 | 55 | 56 | 0 |
| **4:00 AM** | 18.6 | 18.7 | 40 | 41 | 0 | 13.5 | 13.3 | 48 | 50 | 0 | 9.1 | 9.3 | 56 | 57 | 0.1 |
| **4:15 AM** | 18 | 18.1 | 41 | 42 | 0 | 12.1 | 12.1 | 48 | 52 | 0 | 9.1 | 9.3 | 55 | 56 | 0 |
| **4:30 AM** | 17.3 | 17.4 | 41 | 42 | 0 | 9.6 | 9.7 | 52 | 55 | 0 | 9.1 | 9.3 | 55 | 56 | 0.1 |
| **4:45 AM** | 15.6 | 15.7 | 41 | 42 | 0 | 10.1 | 10.2 | 54 | 56 | 0 | 9 | 9.2 | 55 | 56 | 0 |
| **5:00 AM** | 14.1 | 14.2 | 40 | 41 | 0 | 9.2 | 9.3 | 57 | 59 | 0 | 9 | 9.2 | 56 | 57 | 0.1 |
| **5:15 AM** | 13.9 | 14 | 42 | 43 | 0 | 9.5 | 9.6 | 56 | 58 | 0 | 9 | 9.2 | 56 | 57 | 0 |
| **5:30 AM** | 13.8 | 13.9 | 42 | 43 | 0 | 9.9 | 10 | 59 | 60 | 0 | 9.2 | 9.4 | 55 | 56 | 0 |
| **5:45 AM** | 13.8 | 13.9 | 43 | 44 | 0 | 9.4 | 9.7 | 58 | 59 | 0 | 9.6 | 9.8 | 56 | 57 | 0 |
| **6:00 AM** | 14 | 14.1 | 43 | 44 | 0 | 9.2 | 9.4 | 56 | 57 | 0.1 | 9.7 | 9.9 | 57 | 58 | 0 |
| **6:15 AM** | 15.3 | 15.4 | 42 | 43 | 0 | 9.9 | 10 | 60 | 61 | 0 | 9.9 | 10.1 | 58 | 59 | 0 |
| **6:30 AM** | 15.2 | 15.3 | 43 | 44 | 0 | 10.4 | 10.5 | 55 | 56 | 0 | 10.2 | 10.4 | 56 | 57 | 0 |
| **6:45 AM** | 15.8 | 15.9 | 43 | 44 | 0 | 10.9 | 10.9 | 60 | 61 | 0 | 10.6 | 10.8 | 58 | 59 | 0 |
| **7:00 AM** | 16.3 | 16.4 | 43 | 44 | 0 | 11.4 | 11.4 | 58 | 59 | 0 | 11.1 | 11.3 | 57 | 58 | 0.1 |
| **8:00 AM** | 18.7 | 18.6 | 41 | 42 | 0 | 15.2 | 15.2 | 56 | 57 | 0 | 13.6 | 13.7 | 55 | 56 | 0 |

Figure 12 shows the variation in indoor temperature and humidity compared to outdoor conditions during the three days of monitoring. It was observed that during periods of highest radiation (between 10:00 a.m. and 1:00 p.m.), the indoor temperature rose to 33.5 °C on day 1, just 6.7% lower than the outdoor temperature (35.9 °C), which showed direct transmission of solar heat through the corrugated iron. On day 2, the difference was even smaller (3.3%), while on day 3 the transmission decreased slightly to 13.8% less, due to reduced solar radiation and lower ambient temperature range. During the early morning hours (4:00 to 6:00 a.m.), the difference between the interior and exterior was less than 1%, confirming that the system lost the accumulated heat at the same rate as the environment. This phenomenon was explained by the high infrared emissivity of the metal, which favoured the radiation of energy towards the night sky. With regard to humidity, indoor values exceeded the ambient values by between 3% and 5% during the cold hours, reaching 60% RH on day 1 compared to 58% outdoors, and 57% RH on day 2 compared to 56% outdoors.

This increase was associated with internal condensation caused by the low temperature of the metal sheets, which reduced the dew point of the indoor air. The wind speed did

not exceed 0.6 m/s, so heat transfer was predominantly by conduction and radiation, with no significant convective effect. In summary, the figure showed that the model without thermal addition accurately reproduced the variations in the environment, with daytime increases and night-time decreases equivalent to the environment, confirming the high thermal transmittance and low regulation capacity of the base system.

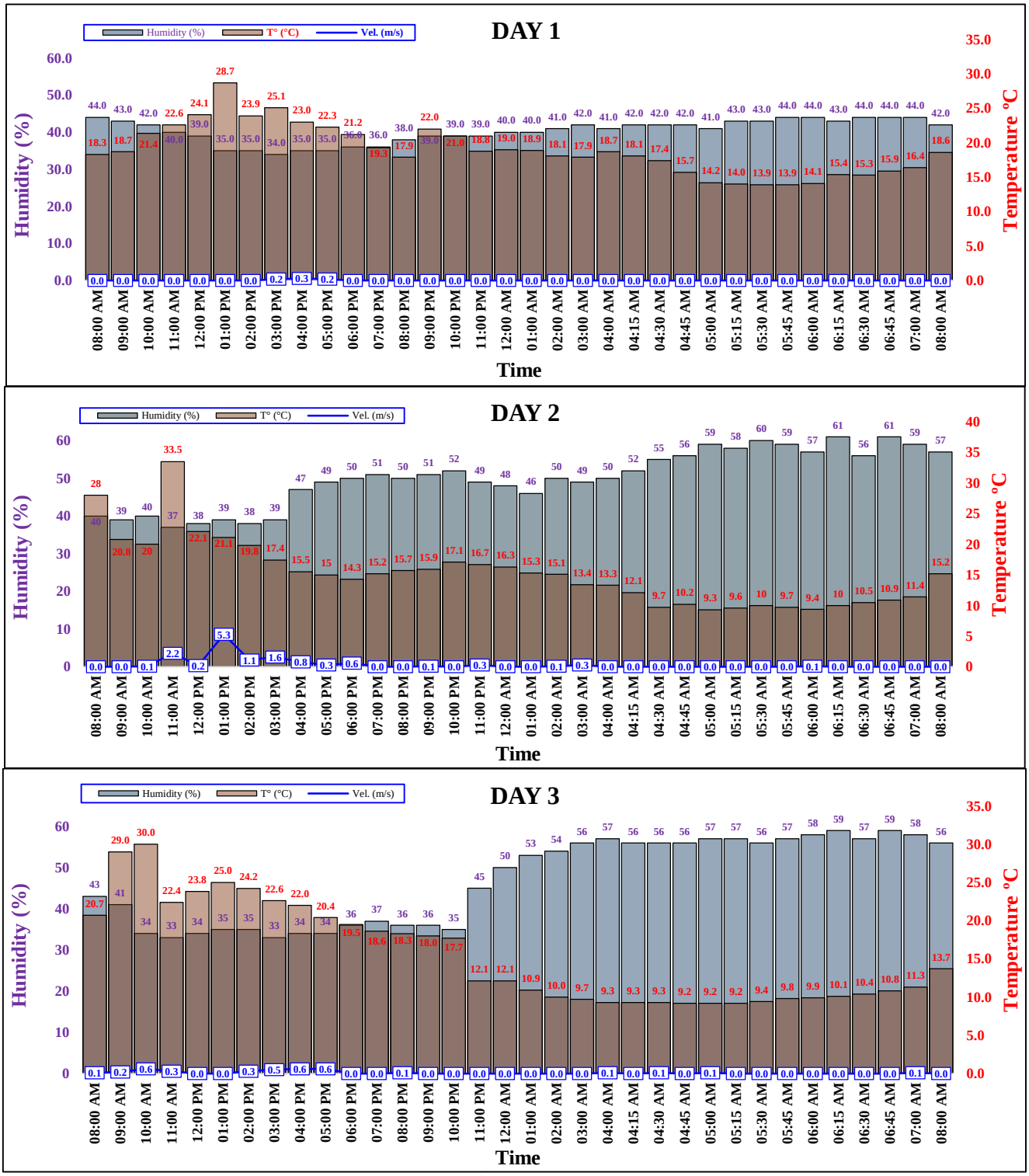


**Fig. 12 Three-day monitoring of the prototype without thermal insulation**

### *4.2. Condition with Ichu Insulation*

*4.2.1. Insulation with 30% Ichu*

Figure 13 shows the thermal behaviour of the prototype with 30% Ichu fiber during continuous monitoring. This model exhibited a more consistent thermal response to external conditions, demonstrating a notable decrease in heat gain during periods of intense solar radiation. The peak indoor temperature of 26 °C at 1:00 p.m. represented a 10% decrease in daytime heat gain when compared to the outdoor ambient temperature of 29 °C. In the coldest period of the night, between 4:30 and 6:00 a.m., indoor temperatures were between 14 °C and 16 °C, while outdoor temperatures fell to 13 °C, demonstrating a thermal retention of approximately 14% when compared to the external environment. This behaviour can be explained by the tubular and porous structure of the ichu fibers. They trap air and serve as a passive insulating medium. This reduces the thermal conductivity of adobe and delays heat loss. In terms of hygrometric performance, the indoor relative humidity ranged from 33% to 43% RH compared to outdoor conditions of 39% - 44% RH. In the early morning hours, however, a slight indoor increase of about 2% was recorded, demonstrating the ability of ichu to absorb and release water vapour, thereby helping to manage moisture without condensation. Overall, the system with 30% ichu had a distinct thermal and hygrometric buffering effect. It reduced daily fluctuations, lessened the heat transfer from the corrugated metal roofing, and provided more stable indoor temperatures at night. This confirms its effectiveness as a natural and sustainable insulating material for improving indoor thermal comfort.

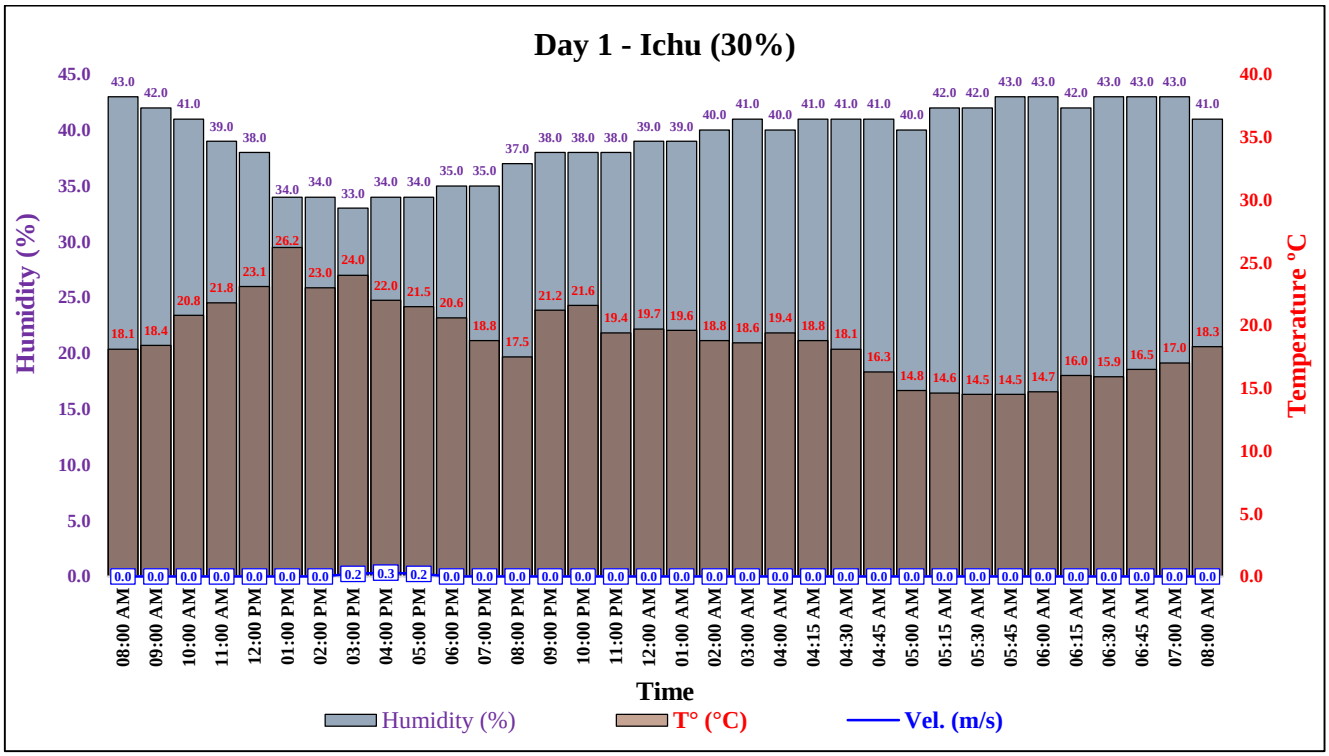


**Fig. 13 Insulation with 30% Ichu**

*4.2.2. Insulation with 33% ichu*

The prototype with 33% ichu fiber showed a more moderate thermal response in comparison to the external environment. The highest indoor temperature recorded was 29.5 °C at 11:00 a.m, with the outdoor temperature reaching 35.9 °C. This results in a 17.8% reduction in daytime heat gain. This reduction in daytime heat gain indicates ichu's contribution in reducing heat transfer through the roof. This is attributed to ichu's fibrous and porous structure, which traps air and reduces thermal conductivity. Indoor temperatures for the coldest period (4:00 to 6:00 a.m.) were between 9.5 °C and 10.5 °C, and the outdoor temperature dropped to 9.2 °C, illustrating a thermal retention of approximately 12% relative to the ambient conditions. This shows the thermal inertia effect of the ichu fibers, where part of the daytime heat was lost during the night. Indoor relative humidity ranged between 46% and 59% RH, which is slightly higher than the outdoor values (45%-58% RH). A slight increase of about 2% was registered during the early morning hours, which can be associated with the hygroscopic nature of ichu. This plant absorbs water vapour at lower temperatures, and as the temperature rises, it releases the water vapour, thereby avoiding internal condensation. Figure 14 shows that the indoor temperature range is narrower due to the delayed heat transfer, as it is more responsive to the surrounding conditions. The use of ichu in the roof is proven to be effective as it minimises heat gain during critical periods and helps the indoor temperature stay more constant.

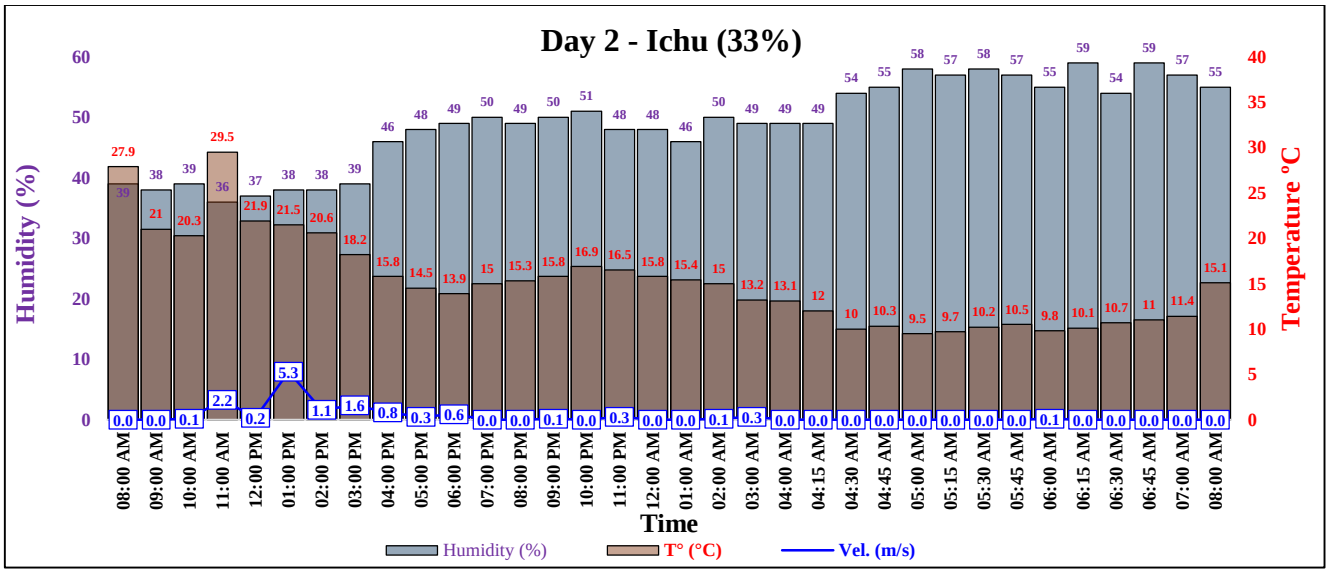


**Fig. 14 Insulation with 33% Ichu**

*4.2.3. Insulation with 36% Ichu*

The prototype with 36% ichu fiber shows an even more accomplished and balanced insulation performance. The indoor temperature, at 10 a.m., was 27.1 °C with an outdoor temperature of 31.3 °C, which is about a 13% reduction in the daytime heat gain. This is explained by the hollow fibrous structure of ichu. The structure of an ichu can be thought of as a natural air layer that helps to reduce thermal conductivity and delay the transfer of heat to the interior space. Considering the time frame of 4:00 to 6:00 a.m., there is little to no solar radiation during this time. During this time span, indoor temperatures were 10°C and 11°C while the outside temperature was 9°C, indicating a heat retention of approximately 11%. This is associated with the lower surface emissivity of the modified systems and the thermal inertia material. The indoor relative humidity was 32% to 57% RH and correlated with the outside relative humidity of 33% to 58% RH. The slightly lower indoor values during the early morning hours do correlate with the partial moisture absorption with ichu fibers, which demonstrates the moderate hygroscopic behaviour. This behaviour is what allows the indoor thermal stability to be maintained and prevents condensation. Figure 15 illustrates the temperature curve of the smother's indoor temperature. There is a notable reduction in amplitude and a reduction in heat transfer. The temperature range has decreased. The incorporation of 36% ichu definitely enhanced the thermal and hygrometric performance of the roof, limiting daytime overheating and improving a stable indoor environment at night without significant moisture accumulation.

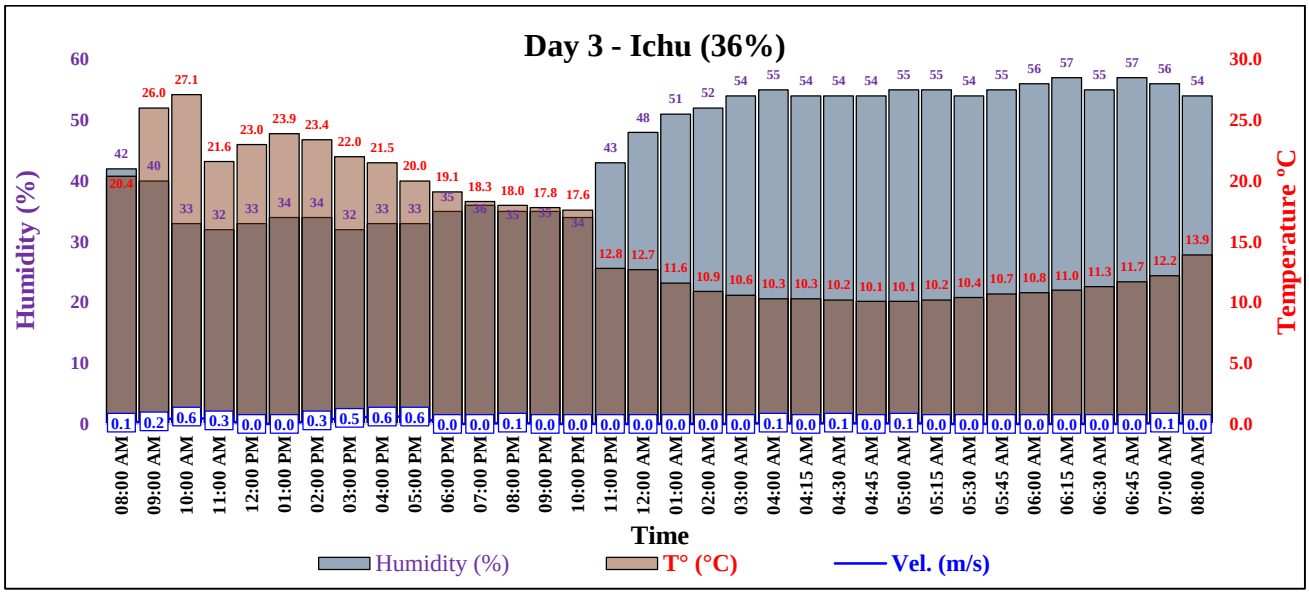


**Fig. 15 Insulation with Ichu at 36%**

### *4.3. Condition with Linen Insulation*

*4.3.1. Insulation with 57% Linen*

The prototype with 57% linen fiber showed a moderate and steady thermal reaction to the outdoor climate. The highest indoor temperature was 24.9 °C at 1:00 p.m. The outdoor temperature was 29.3 °C. This represents a 15% reduction in daytime heat gain. This is due to the high surface density and low thermal conductivity of the linen fibers. The compact cellulosic structure of the linen fibers reduced heat transfer in both conduction and radiation. During solar radiation-absent periods (4:30 to 6:00 a.m.), the indoor temperature was 15 to 16°C, while the outdoor temperature was 13.8°C. This describes a heat retention of around 10%. This correlates with the thermal inertia of the material and its ability to store a portion of the heat that the material builds up during the day. The indoor relative humidity was 31% to 40% RH, and the outdoor was 33% to 43% RH, indicating that indoor moisture was buffered by the linen and microclimate. During peak outdoor humidity hours, this showed that indoor humidity was levelled at 39% to 40%, confirming a lack of water vapour retention. Figure 16 shows how delayed and controlled heat transfer is demonstrated by the indoor temperature curve amplitude. The 57% linen blended fabric incorporated insulations combined with hygroscopic regulation and the natural linen's moisture retention, increased thermal comfort, improved indoor stability, and reduced daily variation in linens.

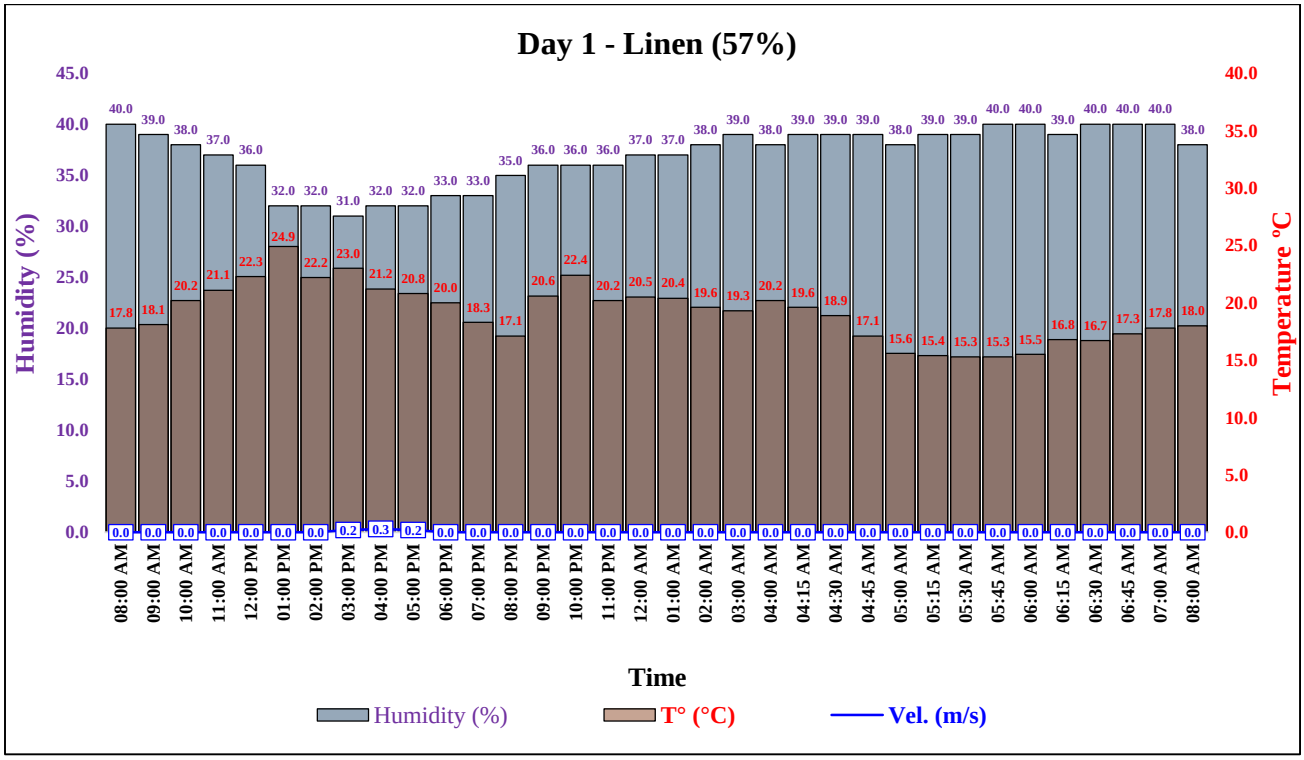


**Fig. 16 Insulation with 57% Linen**

*4.3.2. Insulation with 60% Linen*

The prototype with 60% linen fiber offered good thermal performance against the external environment. At 11:00 a.m, the maximum indoor temperature was 26 °C and the outdoor temperature was 35.9 °C. This is an approximate 27% reduction in daytime heat gain. This is due to the dense fibrous structure of linen and its cellulosic composition, along with an intertwined arrangement of the fibers, which reduces conduction heat transfer and also reflects some of the incident solar radiation. During the coldest period, between 4:30 and 6:00 a.m., indoor temperatures remained between 11.2 °C and 11.8 °C, while the outdoor temperature was 9.2 °C, indicating a heat retention of approximately 22%. This behaviour reflects the thermal inertia of the material, which stores energy during the day and releases it gradually at night. Indoor relative humidity ranged from 34 to 57%. This is similar to the reported outdoor humidity levels of 35 to 60%. During the early morning hours, when humidity is typically 60% outdoors, humidity remained slightly lower at 57% indoors. This demonstrates the hygroscopic regulation by linen fibers, which absorb water vapour and reduce condensation. Indoor temperature curves, especially the one shown in Figure 17, indicate that the variation in amplitude is reduced, confirming the stable and effective control of the temperature fluctuations. Keeping in mind the above, the 60% incorporation of linen is effective. The effective, high-performance insulation is proven once again for plant-based materials.

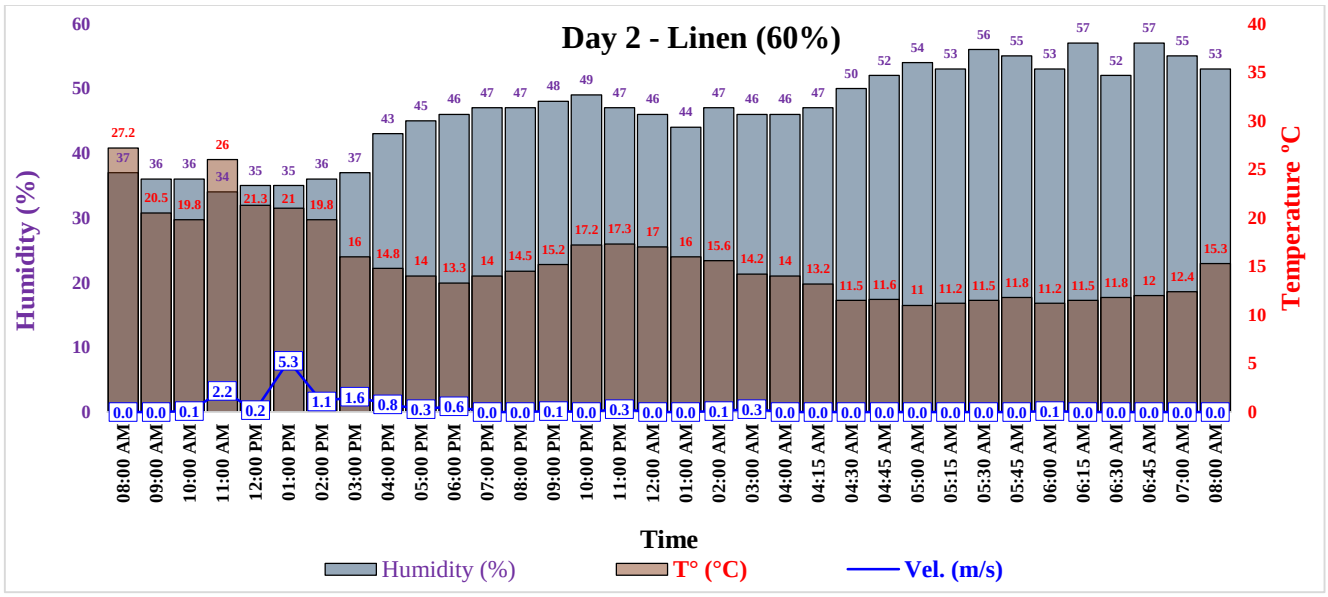


**Fig. 17 Insulation with 60% Linen**

*4.3.3. Insulation with 63% Linen*

Incorporating 63% linen fiber into the prototype showcased negative thermal behaviour, relative to the external environment, which indicates a considerable improvement in insulation performance. Constructed linen fiber is dense, interwoven, and structured. As a result, a compact matrix of low thermal conductivity is made, which limits heat transfer through conduction and reduces internal radiation. During the period of 10:00 a.m. to 11:00 a.m., the indoor temperature was recorded at 25.2 °C, which is a 19.5% reduction in heat gain compared to the outdoor temperature of 31.3 °C. During the period of 3:00 a.m. and 6:00 a.m., indoor temperatures were recorded between 11 °C and 12 °C, while outdoor temperatures were recorded at 9 °C. This indicates a retention of heat of 20%. This is indicative of the material's energy storage and thermal inertia capacity, which allows it to retain and conserve heat throughout the day. The indoor relative humidity varied between 30% and 54% Rh, remaining constantly up to 3 points below the outdoor environment, which demonstrated the absorbent and hygroscopic nature of Linen, capable of capturing part of the ambient water vapour and regulating the internal microclimate. This behaviour reduced the risk of condensation and promoted a drier and more comfortable indoor environment. Figure 18 shows a smoothed interior thermal curve, with a delayed daytime rise and a slower night-time fall. Overall, the use of 63% Linen optimises the thermal and hygrometric balance of the ceiling, limiting daytime heat gain, conserving night-time temperature, and maintaining a controlled humidity level, qualities that consolidate this mixture as one of the most efficient in the system.

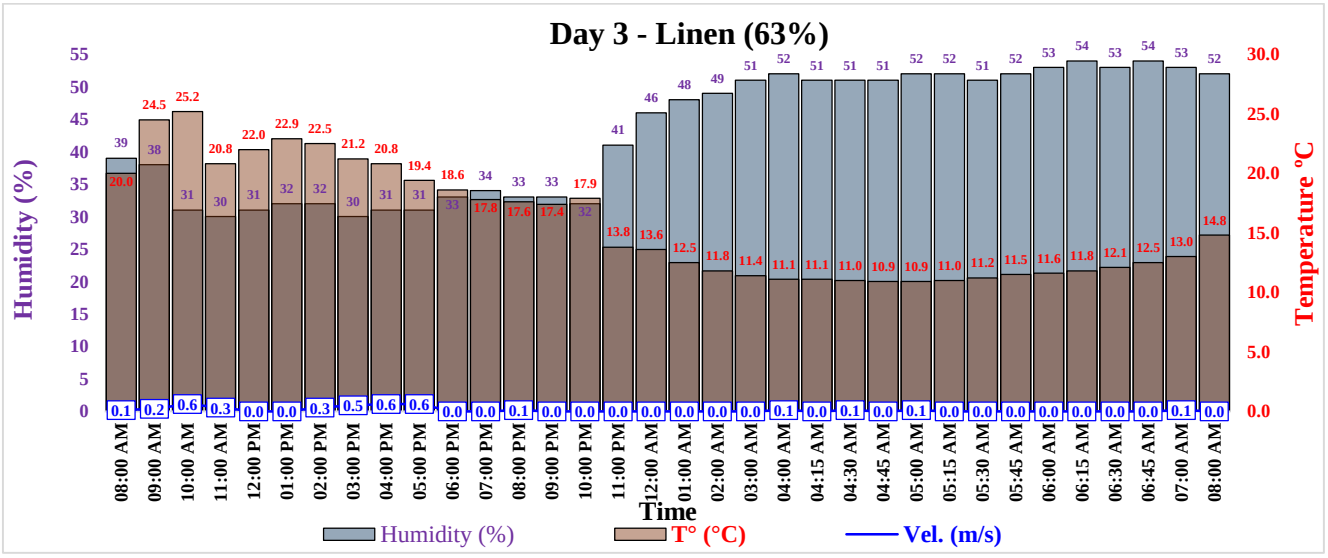


**Fig. 18 Insulation with 63% Linen**

### *4.4. Condition with Activated Carbon from Pineapple Peel Insulation*

*4.4.1. Insulation with 10% Activated Carbon from Pineapple Peel*

The prototype with 10% activated carbon showed a stable thermal response and good damping capacity against external variations. The maximum internal temperature was 23.5 °C at 1:00 p.m., while the external temperature reached 29.3 °C, reflecting a 20% reduction in daytime heat gain. This behaviour was due to the microporous structure of the activated carbon, which generated an absorbent layer capable of retaining air and reducing heat transfer by conduction, as well as reflecting part of the incident radiation. Between 4:30 and 6:00 a.m., indoor temperatures were recorded between 16 °C and 17 °C. At this time, outdoor temperatures fell to 13.8 °C. This indicates a recorded heat retention capacity of 18%. This is associated with the material's energy storage capacity, as activated carbon can gradually release heat. The observed indoor relative humidity levels, which ranged from 29 to 38%, were still lower than the outdoor relative humidity levels of 33 to 43%. The 5% difference can be attributed to the water vapour adsorption of the activated carbon, which can lead to a microclimate that is drier and retains less water. As illustrated in Figure 19, the indoor temperature profile shows a dampened response, characterised by slower heating during the daytime and moderating cooling at night. Overall, the incorporation of 10% activated carbon improved the thermal insulation performance of the roof, reduced daytime heat gains, limited moisture accumulation, and promoted more stable and comfortable indoor conditions over the 24-hour cycle.

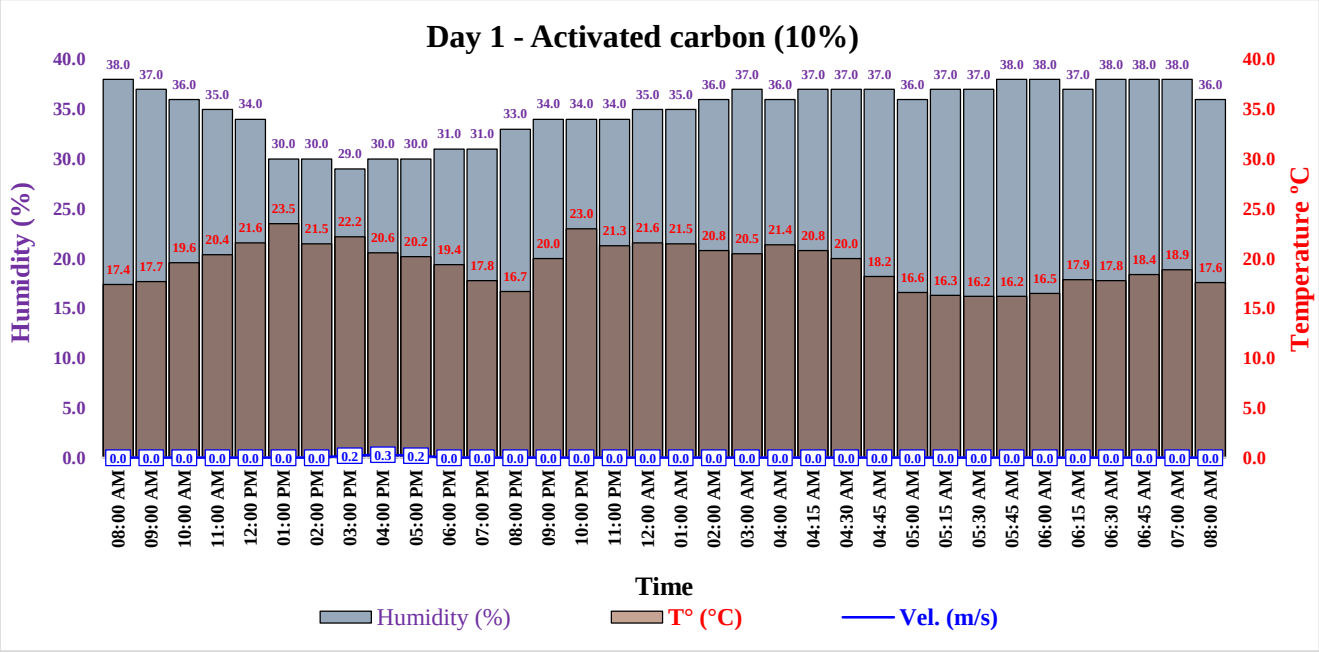


**Fig. 19 Insulation with 10% activated carbon from pineapple peel**

*4.4.2. Insulation with 15% Activated Carbon from Pineapple Peel*

The prototype with 15% activated carbon showed improved thermal performance, exhibiting an interior cooling effect. The coolest indoor temperature recorded was 23.8 °C, with a humidity of 35.9 °C at 11 a.m., representing a 33.7% reduction in heat gain during this time. This cooling can be explained by the microporous structure and the black body heat absorption characteristics of activated carbon. The porous structure of the activated carbon increases absorption of solar radiation and delays the transmission of heat to the interior. This thermal lag effect can be explained by the material's low thermal conductivity and high energy adsorption capacity. When solar radiation was low, at 4, 5, and 6 a.m., the indoor temperatures were held constant at 13 °C, and heat retention was approximately 30%, given an outdoor temperature of 9.2 °C. This phenomenon describes the thermal inertia of the material, which stores and releases heat slowly. The indoor and outdoor relative humidity were 33% to 55% and 35% to 60% RH, respectively. During the 10 a.m. to 11 a.m. hour window, outdoor humidity was above 58%, and indoor humidity was 53% RH, demonstrating that activated carbon does absorb moisture, reducing condensation on the ceiling. As depicted in Figure 20, the indoor temperature curve is more even, demonstrating lower peaks during the day and a more controlled cooling at night. In summary, the addition of 15% activated carbon contributed to greater thermal and hygrometric stability, reducing daytime heat absorption, enhancing night-time heat retention, and providing a more stable, dry, and less variable indoor microclimate.

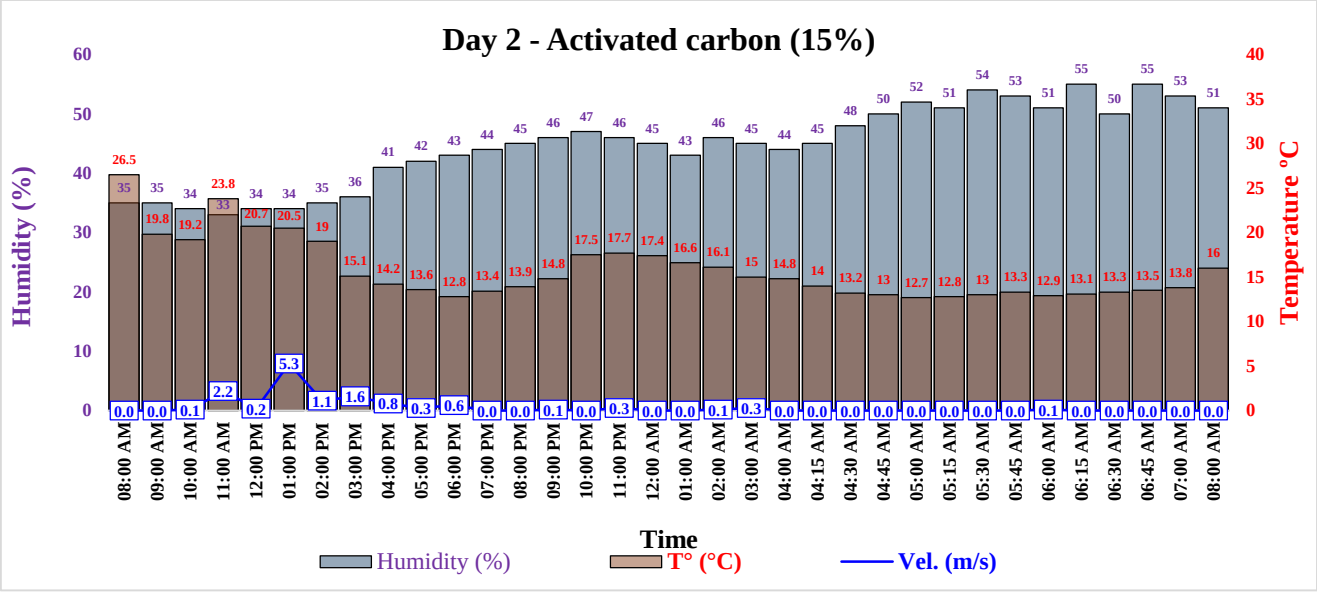


**Fig. 20 Insulation with 15% activated carbon from pineapple peel**

*4.4.3. Insulation with 20% Activated Carbon from Pineapple Peel*

The prototype with 20% activated carbon outperformed both outdoor conditions and the system without additives in thermal performance. The indoor maximum was 23.0 °C at 10:00 a.m., while the outdoor maximum was 31.3 °C, which corresponds to a 26.5% reduction in daytime heat gain. The highly porous structure of activated carbon keeps dry air in the material, lowers the thermal conductivity of the modified adobe, and partially releases heat from solar radiation. During the coldest period, 4:00 to 6:00 a.m., the indoor temperatures were between 12.0 °C and 13.6 °C when outdoors was 9.0 °C, demonstrating approximately 30% thermal retention. This illustrates the material's high heat capacity and energy absorption characteristics, allowing the heat to be released in a gradual and steady manner throughout the night. Indoor relative humidity was between 28% to 52% RH, while it was 33% to 58% RH outdoors, maintaining an average difference of 5%. This reduction correlates with the hygroscopic nature of activated carbon, which lowers the water vapour levels in the air and serves to prevent ceiling condensation. As shown in Figure 21, the indoor temperature profile exhibits a smoother response, with attenuated daytime peaks and more gradual nocturnal cooling, indicating a clear reduction in temperature amplitude. Overall, the incorporation of 20% activated carbon provided enhanced thermal and hygrometric performance by reducing daytime heat gains, retaining heat during the early morning hours, and maintaining a drier and more stable indoor environment, thereby confirming its effectiveness as a passive insulating and environmental regulation component within the roofing system.

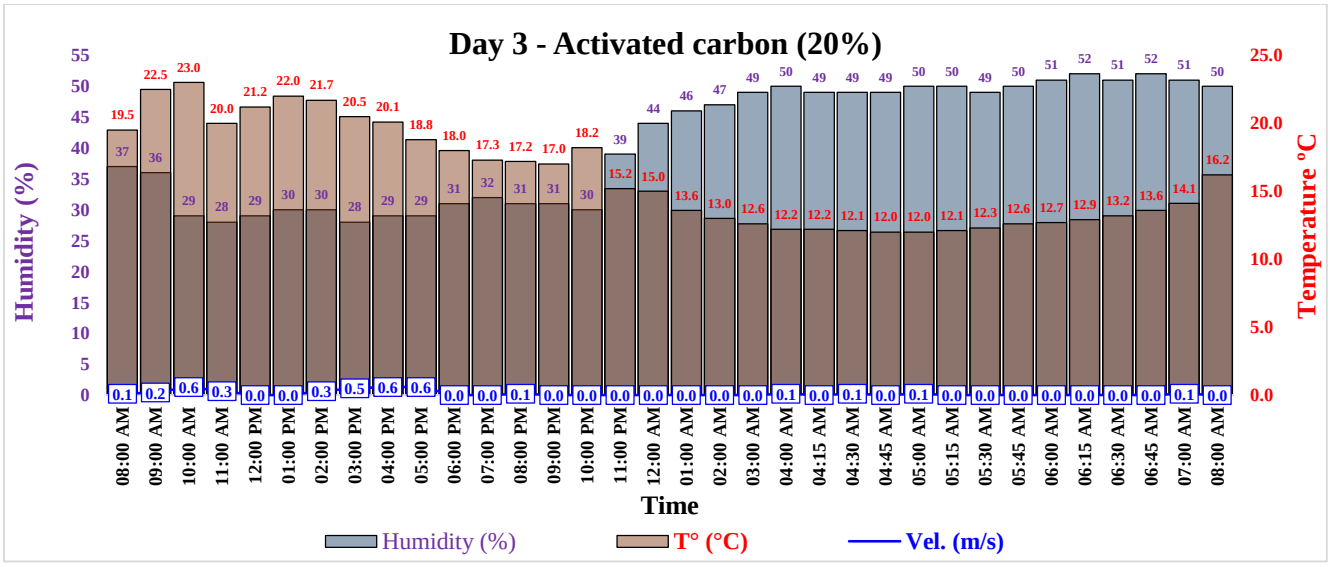


**Fig. 21 Insulation with 20% activated charcoal from pineapple peel**

### *4.5. Optimal Additions*

*4.5.1. Comparison based on Temperature (°)*

Table 6 shows the optimum dosages as 33% ichu, 60% linen, and 20% activated carbon, as these provided the highest overall thermal efficiency and balanced insulation, heat retention, and structural stability. A maximum thermal efficiency of 21.69% was recorded for the 33% ichu mixture at 11:00 am. This indicates a significant drop in indoor temperature in comparison to the outdoor temperature. This is explained by the uniform distribution of fibres in the adobe matrix, which created micro-scale pores that minimised thermal conductivity and maintained cohesion of the material as well as prevented excessive porosity and cracking. Consequently, ichu acted as a good plant-based insulator with thermal inertia and without the negative impact on indoor humidity. Among the plant-based additives, the mixture with 60% linen recorded the highest thermal efficiency of 38.08% at 11:00 am. This was caused by the low thermal conductivity and reflecting capacity of the lign, which assisted in heat loss. At this ratio, the optimum balance of thermal mass and air permeability was achieved, which decreased daytime heat gain and kept the indoor temperatures stable during the early morning hours. The behaviours documented, while demonstrating some advantages, resulted in a trackable thermal and humidity damping and uniformity. Lastly, the addition of 20% activated carbon achieved the highest overall thermal efficiency of 50.84%, occurring at 11:00 am. This value translates to a reduction of greater than 50% of the heat conveyed to the interior. This is considering activated carbon's high porosity and specific surface area, allowing for the dual function of adsorbing and regulating (thermally and hygrometrically) the solar radiation and water vapour. As a result, indoor temperatures during early hours remained the same (12-14 °C) and a drier internal environment was preserved through the heat and moisture buffering. In contrast to lower concentrations (10% and 15%), the 20% dosage was at an optimal saturation level, and insulation performance was maximised without compromising the structural integrity of the roofing system.

**Table 6. Temperature (°C)**

| Time | Day 1 | | | Day 2 | | | Day 3 | | |
|---|---|---|---|---|---|---|---|---|---|
| | Ichu (30%) % Efficiency | Linen (57%) % Efficiency | Activated Carbon (10%) % Efficiency | Ichu (33%) % Efficiency | Linen (60%) % Efficiency | Activated Carbon (15%) % Efficiency | Ichu (36%) % Efficiency | Linen (63%) % Efficiency | Activated Carbon (20%) % Efficiency |
| **8:00 AM** | 1.66% | 3.37% | 5.75% | 1.08% | 3.68% | 6.42% | 1.96% | 4.00% | 6.67% |
| **9:00 AM** | 2.17% | 3.87% | 6.21% | 1.43% | 0.98% | 4.55% | 15.77% | 22.86% | 33.78% |
| **10:00 AM** | 4.33% | 7.43% | 10.71% | 1.97% | 0.51% | 3.65% | 15.50% | 24.21% | 36.09% |
| **11:00 AM** | 5.05% | 8.53% | 12.25% | 21.69% | 38.08% | 50.84% | 5.56% | 9.62% | 14.00% |
| **12:00 PM** | 5.63% | 9.42% | 12.96% | 2.74% | 5.63% | 8.70% | 5.22% | 10.00% | 14.15% |
| **1:00 PM** | 11.83% | 17.67% | 24.68% | 2.33% | 0.00% | 2.44% | 5.86% | 10.48% | 15.00% |
| **2:00 PM** | 5.22% | 9.01% | 12.56% | 5.34% | 1.52% | 2.63% | 4.70% | 8.89% | 12.90% |
| **3:00 PM** | 6.25% | 10.87% | 14.86% | 7.14% | 5.62% | 11.92% | 4.09% | 8.02% | 11.71% |
| **4:00 PM** | 5.91% | 9.91% | 13.11% | 3.16% | 3.38% | 7.75% | 3.72% | 7.21% | 10.95% |
| **5:00 PM** | 5.12% | 8.65% | 11.88% | 6.21% | 10.00% | 13.24% | 3.00% | 6.19% | 9.57% |
| **6:00 PM** | 3.88% | 7.00% | 10.31% | 5.04% | 9.77% | 14.06% | 2.62% | 5.38% | 8.89% |
| **7:00 PM** | 3.19% | 6.01% | 8.99% | 2.00% | 9.29% | 14.18% | 2.19% | 5.06% | 8.09% |
| **8:00 PM** | 2.86% | 5.26% | 7.78% | 3.92% | 9.66% | 14.39% | 2.22% | 4.55% | 6.98% |
| **9:00 PM** | 5.19% | 8.25% | 11.50% | 0.63% | 4.61% | 7.43% | 1.69% | 4.02% | 6.47% |
| **10:00 PM** | 3.24% | 6.70% | 9.13% | 2.37% | 0.58% | 1.14% | 0.57% | 1.12% | 2.75% |
| **11:00 PM** | 3.61% | 7.43% | 12.21% | 1.82% | 2.89% | 5.08% | 6.25% | 13.04% | 21.05% |
| **12:00 AM** | 4.06% | 7.80% | 12.50% | 5.06% | 2.35% | 4.60% | 5.51% | 11.76% | 20.00% |
| **1:00 AM** | 4.08% | 7.84% | 12.56% | 1.30% | 5.00% | 8.43% | 7.76% | 14.40% | 21.32% |
| **2:00 AM** | 4.26% | 8.16% | 13.46% | 1.33% | 2.56% | 5.59% | 9.17% | 16.10% | 23.85% |
| **3:00 AM** | 4.30% | 7.77% | 13.17% | 3.03% | 4.23% | 9.33% | 10.38% | 16.67% | 24.60% |
| **4:00 AM** | 4.12% | 7.92% | 13.08% | 3.05% | 3.57% | 8.78% | 11.65% | 18.02% | 25.41% |
| **4:15 AM** | 4.26% | 8.16% | 13.46% | 0.83% | 8.33% | 13.57% | 11.65% | 18.02% | 25.41% |
| **4:30 AM** | 4.42% | 8.47% | 13.50% | 4.00% | 16.52% | 27.27% | 10.78% | 17.27% | 24.79% |
| **4:45 AM** | 4.29% | 8.77% | 14.29% | 1.94% | 12.93% | 22.31% | 10.89% | 17.43% | 25.00% |
| **5:00 AM** | 4.73% | 9.62% | 15.06% | 3.16% | 16.36% | 27.56% | 10.89% | 17.43% | 25.00% |
| **5:15 AM** | 4.79% | 9.74% | 14.72% | 2.06% | 15.18% | 25.78% | 11.76% | 18.18% | 25.62% |
| **5:30 AM** | 4.83% | 9.80% | 14.81% | 2.94% | 13.91% | 23.85% | 11.54% | 17.86% | 25.20% |
| **5:45 AM** | 4.83% | 9.80% | 14.81% | 10.48% | 20.34% | 29.32% | 10.28% | 16.52% | 23.81% |
| **6:00 AM** | 4.76% | 9.68% | 15.15% | 6.12% | 17.86% | 28.68% | 10.19% | 16.38% | 23.62% |
| **6:15 AM** | 4.38% | 8.93% | 14.53% | 1.98% | 13.91% | 24.43% | 10.00% | 16.10% | 23.26% |
| **6:30 AM** | 4.40% | 8.98% | 14.61% | 2.80% | 11.86% | 21.80% | 9.73% | 15.70% | 22.73% |

| | | | | | | | | | |
|---|---|---|---|---|---|---|---|---|---|
| **6:45 AM** | 4.24% | 8.67% | 14.13% | 0.91% | 9.17% | 19.26% | 9.40% | 15.20% | 22.06% |
| **7:00 AM** | 4.12% | 8.43% | 13.76% | 0.00% | 8.06% | 17.39% | 9.02% | 14.62% | 21.28% |
| **8:00 AM** | 2.19% | 3.89% | 6.25% | 0.66% | 0.65% | 5.00% | 2.16% | 8.11% | 16.05% |

*4.5.2. Comparison based on Humidity (%RH)*

The monitoring results from the three experimental days, as summarised in Table 7, reflect the noticeable variation in thermal efficiency (%) among the various roof systems incorporating plant fibres versus those with activated carbon. Each of the materials was observed to perform optimally at different specific dosages. Ichu, for example, reached its optimum at 33% (Day 2) at a thermal efficiency of 9.68% at 1 p.m. This proportion added to the overall performance of Ichu, resulting in a more compact internal structure in comparison to the 30% mixture. This promoted internal thermal conductivity to decrease as the still air trapping potential in the fibrous network improved. Furthermore, the thermal efficiency was less variable but relatively consistent from midday to 4 p.m. This indicates a thermal response, for which this internal thermal structure has delayed peak temperatures. Ichu's performance for the sustained insulative effect was attributable to moderate fibrous network porosity. This also complemented the still air trapping potential in the network. Linen also recorded its optimum at 60% (Day 2) of thermal efficiency, 7.69% during the early morning (6:15 a.m. to 8:00 a.m.), and exhibited sustained efficiency in the afternoon. This performance, associated with the fibrous structure of linen, is laminar and is useful in dispersing incident solar radiation to keep the absorption low. At this proportion, a dense fibrous barrier was formed, retaining dry air and reducing the thermal gradient between the exterior and the interior. In relation to ichu, linen demonstrated more consistent behaviour at night, which confirms its ability to passively store heat and gradually release it. Activated carbon, at a dosage of 20% (Day 3), achieved the best overall thermal performances, with a maximum of 13.89% at 8:00 a.m. and an average of 12.4% for the day. This superior performance to all other plant-based additives illustrates the considerable thermal and hygrometric regulation potential of activated carbon. Its microstructure, which is very porous, encourages the absorption of solar radiation, which is then controlled during the night. Additionally, the surface adsorption of water vapour diminished hygrometric variability which contributes to a more stable indoor environment.

**Table 7. Humidity (%RH) at critical times**

| Time | Day 1 | | | Day 2 | | | Day 3 | | |
|---|---|---|---|---|---|---|---|---|---|
| | **Ichu (30%) % Efficiency** | **Linen (57%) % Efficiency** | **Activated Carbon (10%) % Efficiency** | **Ichu (33%) % Efficiency** | **Linen (60%) % Efficiency** | **Activated Carbon (15%) % Efficiency** | **Ichu (36%) % Efficiency** | **Linen (63%) % Efficiency** | **Activated Carbon (20%) % Efficiency** |
| **8:00 AM** | 4.88% | 7.50% | 13.16% | 2.56% | 2.70% | 8.57% | 5.00% | 7.69% | 13.51% |
| **9:00 AM** | 5.00% | 7.69% | 13.51% | 0.00% | 5.56% | 8.57% | 2.56% | 5.26% | 11.11% |
| **10:00 AM** | 2.50% | 7.89% | 13.89% | 2.56% | 5.56% | 11.76% | 3.13% | 6.45% | 13.79% |
| **11:00 AM** | 5.41% | 5.41% | 11.43% | 2.78% | 2.94% | 6.06% | 3.23% | 6.67% | 14.29% |
| **12:00 PM** | 5.56% | 5.56% | 11.76% | 0.00% | 5.71% | 8.82% | 0.00% | 6.45% | 13.79% |
| **1:00 PM** | 9.68% | 6.25% | 13.33% | 2.63% | 5.71% | 8.82% | 3.03% | 6.25% | 13.33% |
| **2:00 PM** | 6.25% | 6.25% | 13.33% | 2.63% | 2.78% | 5.71% | 0.00% | 6.25% | 13.33% |
| **3:00 PM** | 3.13% | 6.45% | 13.79% | 5.13% | 0.00% | 2.78% | 3.23% | 6.67% | 14.29% |
| **4:00 PM** | 3.03% | 6.25% | 13.33% | 2.17% | 4.65% | 9.76% | 3.13% | 6.45% | 13.79% |
| **5:00 PM** | 6.25% | 6.25% | 13.33% | 2.08% | 4.44% | 11.90% | 0.00% | 6.45% | 13.79% |
| **6:00 PM** | 9.38% | 6.06% | 12.90% | 2.04% | 4.35% | 11.63% | 2.94% | 6.06% | 12.90% |
| **7:00 PM** | 2.94% | 6.06% | 12.90% | 2.00% | 4.26% | 11.36% | 0.00% | 5.88% | 12.50% |
| **8:00 PM** | 5.71% | 5.71% | 12.12% | 0.00% | 4.26% | 8.89% | 2.94% | 6.06% | 12.90% |
| **9:00 PM** | 2.70% | 5.56% | 11.76% | 2.00% | 2.08% | 6.52% | 6.06% | 6.06% | 12.90% |
| **10:00 PM** | 5.56% | 5.56% | 11.76% | 1.96% | 2.04% | 6.38% | 3.03% | 6.25% | 13.33% |
| **11:00 PM** | 2.70% | 5.56% | 11.76% | 2.08% | 0.00% | 2.17% | 4.76% | 7.32% | 12.82% |
| **12:00 AM** | 5.41% | 5.41% | 11.43% | 2.08% | 2.17% | 4.44% | 4.26% | 6.52% | 11.36% |
| **1:00 AM** | 2.63% | 5.41% | 11.43% | 2.17% | 2.27% | 4.65% | 4.00% | 8.33% | 13.04% |
| **2:00 AM** | 2.56% | 5.26% | 11.11% | 2.00% | 4.26% | 6.52% | 1.92% | 8.16% | 12.77% |
| **3:00 AM** | 5.13% | 5.13% | 10.81% | 2.04% | 4.35% | 6.67% | 1.85% | 7.84% | 12.24% |
| **4:00 AM** | 2.56% | 5.26% | 11.11% | 2.04% | 4.35% | 9.09% | 3.70% | 7.69% | 12.00% |
| **4:15 AM** | 5.13% | 5.13% | 10.81% | 2.04% | 2.13% | 6.67% | 3.77% | 7.84% | 12.24% |
| **4:30 AM** | 5.13% | 5.13% | 10.81% | 3.70% | 4.00% | 8.33% | 1.85% | 7.84% | 12.24% |
| **4:45 AM** | 7.89% | 5.13% | 10.81% | 1.82% | 3.85% | 8.00% | 5.77% | 7.84% | 12.24% |
| **5:00 AM** | 2.56% | 5.26% | 11.11% | 1.72% | 5.56% | 9.62% | 1.82% | 7.69% | 12.00% |

| | | | | | | | | | |
|---|---|---|---|---|---|---|---|---|---|
| **5:15 AM** | 2.44% | 7.69% | 13.51% | 1.75% | 5.66% | 9.80% | 3.70% | 7.69% | 12.00% |
| **5:30 AM** | 5.00% | 7.69% | 13.51% | 1.72% | 5.36% | 9.26% | 3.77% | 7.84% | 12.24% |
| **5:45 AM** | 2.38% | 7.50% | 13.16% | 1.75% | 5.45% | 9.43% | 3.70% | 7.69% | 12.00% |
| **6:00 AM** | 4.88% | 7.50% | 13.16% | 1.82% | 5.66% | 9.80% | 1.79% | 7.55% | 11.76% |
| **6:15 AM** | 7.69% | 7.69% | 13.51% | 1.69% | 5.26% | 9.09% | 5.45% | 7.41% | 11.54% |
| **6:30 AM** | 2.38% | 7.50% | 13.16% | 1.85% | 5.77% | 10.00% | 3.70% | 5.66% | 9.80% |
| **6:45 AM** | 7.50% | 7.50% | 13.16% | 1.69% | 5.26% | 9.09% | 3.57% | 7.41% | 11.54% |
| **7:00 AM** | 4.88% | 7.50% | 13.16% | 1.75% | 5.45% | 9.43% | 3.64% | 7.55% | 11.76% |
| **8:00 AM** | 5.13% | 7.89% | 13.89% | 1.82% | 5.66% | 9.80% | 1.85% | 5.77% | 10.00% |

*4.5.3. Comparison based on Wind Speed*

The wind speed on the three days of the experiment remained relatively the same. Values were generally below 0.6 m/s, indicating the presence of a laminar flow without the roof surface flow turbulence. This condition allowed the evaluation of the thermal effect of the material addition without the impact of external convection. On Day 1, some wind speed peaks isolated up to 5.3 m/s were recorded between 1:00 and 2:00, and these were aligned with the solar gains at the time. This caused a surface convective heat exchange to drop the indoor temperature. For roofs with ichu and linen, this effect was negligible as the fibrous material was a micro-scale flow dissipater that reduced direct convective heat transfer. For Day 2, the average speed was 0.2 m/s, which indicates stability of the atmosphere. Under such conditions, the thermal performance of the mixtures was dominated by conduction and radiation. This clearly demonstrated the insulating effect of Ichu at 33% and Lino at 60%. Finally, on Day 3, the wind speed remained almost constant at around 0.1 m/s, creating ideal thermal calm conditions for evaluating night-time heat retention. Under these conditions, the 20% activated carbon showed superior thermal stability, minimising convective dissipation and better conserving accumulated heat. Overall, the low incidence of wind on all days confirmed that the thermal variations recorded were mainly attributed to the intrinsic properties of the materials, reaffirming the passive efficiency of the improved roofs in the face of external fluctuations in the atmospheric environment.

## 5. Recommendations

Firstly, the validity of using scale models in research into the thermal and structural behaviour of adobe houses is based on the principles of geometric similarity, material similarity, and boundary conditions, which are widely recognised in experimental engineering [79]. Various studies have shown that reduced models can accurately reproduce the behaviour of real structures when the proportionality between dimensions, thermal properties, and energy exchange conditions is maintained. This allows the results of temperature, damping, and thermal lag obtained in prototypes to be extrapolated to full-scale buildings, provided that the equivalence of form, materials, and thicknesses is respected [80, 81]. In this context, the prototype developed is representative, as it preserves the geometric relationship of traditional rural dwellings, uses local materials, and reproduces the typical construction system with a corrugated iron roof and improved adobe thermal mass, under controlled environmental conditions. For this reason, the results obtained are scientifically valid and can be applied to the actual design of sustainable bioclimatic dwellings, following the criteria of physical similarity indicated in the specialised literature.

Secondly, the incorporation of additives and reinforcements in adobe mixtures has proven to be an effective strategy for improving their strength, durability, and crack control. Stabilisation and reinforcement techniques using natural or synthetic fibres or meshes contribute significantly to reducing shrinkage cracks and improving the mechanical performance of the material [82]. In particular, the application of external or intermediate reinforcement meshes in adobe walls and blocks increases compressive strength and structural integrity by distributing internal stresses and preventing crack propagation [83, 84]. In the context of mixtures modified with activated carbon, although this additive improves the thermal efficiency and densification of adobe, it can induce surface brittleness; therefore, the inclusion of an intermediate mesh is technically justified, as it acts as a complementary mechanical reinforcement that prevents cracking and ensures a more stable and durable behaviour of the composite material, as shown in Figure 22.

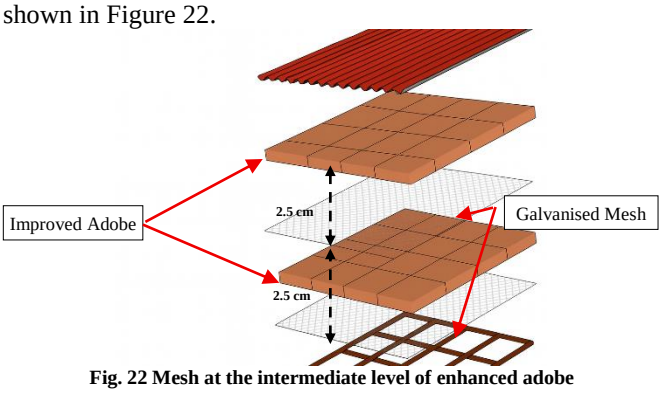


**Fig. 22 Mesh at the intermediate level of enhanced adobe**

## 6. Discussion

According to research conducted by Montoya, the implementation of biothermal panels with Ichu fibre, barley straw, and plaster with a thickness of 5 cm allowed a minimum temperature of 0.7 °C with 61.6 %RH to be achieved, while the panel made with Ichu, barley straw, and clay reached 1.1 °C with 63.9% Rh. Compared to the condition without

insulation (−1.0 °C and 65.9% Rh), both achieved thermal improvements of 1.7 °C and 1.1 °C, respectively, validating Ichu as an effective insulator in high Andean conditions [53]. In this study, activated carbon at 20%, which reached a minimum internal temperature of 12.0 °C compared to an external temperature of 9.0 °C, achieved a difference of +3.0 °C and a reduction in humidity of 4 percentage points at 1:00 pm; 60% Linen, which recorded an internal temperature of 11.0 °C (+2.0 °C compared to the external temperature) with a 2-point decrease in humidity; and 33% Ichu, with an internal temperature of 9.5 °C (+0.5 °C above the external temperature) and a slight hygroscopic tendency (+1 point). The results show that the combination of plant fibres and activated carbon improves thermo-hygrometric comfort by insulating heat and thus increasing indoor temperatures during the coldest hours, while also decreasing the moisture level. Of the materials examined, activated carbon demonstrated the most significant impact in thermal adsorption and vapour control, linen provided thermal inertia and balanced capillary action, and ichu acted mainly as an insulating material due to its porosity. Altogether, these contributions made a positive impact on the sustainable roofing system's efficiency and performance. A major difference, in relation to previous research, pertains to construction style, as Montoya used multilayer panel systems with plaster or clay binders, while in this study, the variable material percentages were incorporated directly into the adobe matrix below metal roofing, which affected the insulation and humidity control results.

In a related experimental study, Chea Gonzales noted that the addition of ichu fibre at approximately 4% of the weight of mortars and blocks lowered thermal conductivity to 0.25 W/m·K, thus surpassing conventional mixtures without additives. Nevertheless, parameters of more than 6% caused a decrease in density and mechanical strength, and therefore, an inadequate structural applicability [23]. Conversely, this study examined even higher ichu levels (30%, 33%, and 36%) directly incorporated into modified adobe roofing systems, resulting in minimum indoor temperatures of 14.8 °C, 9.5 °C, and 10.1 °C, respectively, while the average outdoor temperature was 9.0 °C. These values represent temperature increases of +5.8 °C, +0.5 °C, and +1.1 °C, respectively, thus corroborating the fact that ichu is effective as a natural insulating material, especially in the case of the 33% ichu content, where there was an optimal combination of thermal insulation and hygrometric stability. This difference is mostly attributed to the scope or the role of ichu. While Chea used the fibre as a dispersed additive within a cementitious matrix in order to reduce thermal conductivity, the present study used ichu in the form of a high-volume fibrous element incorporated within the roofing system, thereby enhancing the ability of the system to trap air and increasing thermal resistance during nighttime. Even with these methodological differences, both studies reflect that ichu performs best within optimal dosages that balance insulation efficiency and material retention, reflecting the adaptability of different construction approaches in the high Andean dwellings.

El Messiry et al. state that the insulating panels manufactured from linen waste reach thermal conductivities of 0.0298 to 0.325 W/m·K and the one achieving the best performance was the panel with 60% linen fibre and 40% natural binder, modified with paraffin and reflective layers, which obtained 0.0298 W/m·K, thus exceeding even some of the conventional materials, such as mineral wool and expanded polystyrene [27]. In this study, the incorporation of Linen into modified adobe roofs showed that the optimal dose was 60%, reaching a minimum indoor temperature of 11.0 °C compared to 9.0 °C outdoors, representing a temperature increase of +2.0 °C and a reduction in relative humidity of 2 points compared to the environment. At adjacent doses (57% and 63%), the differences were +6.6 °C and +1.9 °C, confirming that 60% best balances thermal insulation, structural stability, and hygrometric control. The difference in magnitude compared to El Messiry's study is due to the experimental approach: while his work prioritised fibre compaction and the inclusion of multi-layer layers to reduce conductivity, in this study, the Linen was integrated directly into the roof matrix under metal roofing. Yet both results show that linen, due to its structure of low-density fibres and air retention, acts as an effective and sustainable thermal insulator for rural dwellings.

Según Tonelli et al. el uso de escoria granulada de alto horno (GGBS) activada con nanopartículas de hidróxido de calcio permitió consolidar adobes al reducir su porosidad del 10 % al 5 % y duplicar el coeficiente de abrasión, además de disminuir el índice de decohesión de 0.75 a 0.37 mg/cm² [32]. This clearly demonstrates the importance of high surface area and reactive additives in the strengthening and stabilising of porous materials. Regarding the modified adobe roofs, activated carbon produced the best thermal results, attaining an indoor temperature of 12.0 °C with an outdoor temperature of 9.0 °C at the optimum dosage of 20%. This represents a thermal gain of +3.0 °C and a drop in indoor relative humidity of 4%. At lower proportions (10% and 15%), the thermal differences were +7.6 °C and +3.7 °C, respectively, confirming that increasing the volume of charcoal improves thermal insulation, although its effectiveness stabilises at 20%. The difference is that while Tonelli sought mechanical consolidation of adobe bricks, this study prioritised thermal insulation, although in both cases the strategy converges on the use of finely divided additives that enhance the durability and comfort of sustainable constructions.

## 7. Practical Implications, Limitations, and Future Work

The findings of this study provide a technically grounded basis for enhancing the thermal performance of adobe roofing systems in high-Andean housing exposed to frost conditions. The incorporation of ichu fibre, flax fibre, and activated

carbon modifies the thermo-hygrometric behaviour of the building envelope by increasing thermal resistance, improving heat retention during nocturnal cooling, and contributing to moisture regulation. Given their local availability, low economic cost, and compatibility with traditional earthen construction, these materials constitute a viable passive strategy for improving indoor environmental conditions without reliance on external energy inputs. From an innovation standpoint, the study provides a controlled, comparative evaluation of three sustainable additives under equivalent experimental conditions, enabling a consistent assessment of their relative performance. Moreover, the direct integration of these materials into the adobe roofing matrix, rather than their conventional application as independent insulating systems, represents a methodological and practical contribution with direct relevance to real-scale construction in vulnerable high-altitude contexts.

Despite the consistency of the results obtained, certain limitations inherent to the experimental approach must be acknowledged. The study was conducted under real environmental conditions, which, while enhancing the representativeness of the results, also introduces variability associated with external climatic factors such as temperature fluctuations, solar radiation, and ambient humidity. Although efforts were made to ensure comparability between test configurations, these uncontrolled variables may influence the thermal response of the evaluated systems. In addition, the assessment focused primarily on short-term thermo-hygrometric performance, without addressing long-term aspects such as material durability, degradation, and seasonal variability. Consequently, future research should prioritise extended monitoring under different climatic scenarios, as well as full-scale implementation to further validate the performance of these systems in real housing conditions. Further investigations are also recommended to evaluate long-term mechanical behaviour, material stability, and the potential combined use of these additives to optimise the overall performance of adobe-based roofing systems in high-Andean environments.

## 8. Conclusion

Firstly, the research confirmed that incorporating local materials such as ichu, linen, and activated charcoal from pineapple peel into modified adobe roofs is an effective strategy for improving thermal comfort in high Andean dwellings. The integration of these additives made it possible to mitigate night-time energy losses and reduce relative humidity, which are critical conditions in frosty environments. Overall, the findings validate the viability of using plant fibers and agro-industrial waste as sustainable, replicable, and low-cost inputs for rural construction.

Secondly, it was determined that the optimal addition of ichu fibre corresponds to 33%, the level at which the material achieved its best thermal-hygrometric performance within the roofing system. This percentage allowed for controlled heat transfer during the coldest hours, demonstrating an effective capacity to store thermal energy in its fibrous structure without altering the stability of the adobe. Above this threshold, such as at 36%, performance became less efficient: the matrix lost compactness, internal cohesion decreased, and moisture absorption increased slightly, reducing the net insulating capacity of the assembly. In contrast, lower proportions failed to retain heat in any appreciable way. Thus, ichu proved to be a traditionally valid insulator, whose potential depends on fine-tuning the dosage to balance thermal porosity with the mechanical strength of the roof.

Thirdly, with the exception of ichu, the rather stiff thermal behaviour of linen fibre is due to its structure, compactness, low density, and high heat capacity, which facilitate thermal absorption and release at slower rates. The most efficient dosage was the 60% that kept indoor temperatures and relative humidity more stable than the outdoor conditions. Thermal behaviour was not uniform when the proportion was reduced to 57% and increased to 63%. The thinner layers did not retain sufficient energy, and the thicker, denser layers restricted the movement of air within the layer, and therefore, the energy buffering capacity to accommodate the daily changes was diminished. Thus, linen was identified as having balanced thermal behaviour as an insulator that positively contributes to the microclimate by avoiding and not just dampening specific heat gain. The insulator stabilised the microclimate during the day and night temperature fluctuations.

Fourthly, among the evaluated formulations, the addition of activated carbon from the pineapple peel proved to be the most effective, merging thermal insulation with hygrometric control, all within the same construction system. An optimal dosage of 20% provided a stable indoor temperature of 12 °C, which is 3 °C above the outside temperature, and a relative humidity reduction of about 4 percentage points, resulting in a warmer and drier indoor environment during the critical hours of the early morning. Unlike the lower proportions (10% and 15%), which showed specific thermal improvements but less night-time stability, the mixture with 20% addition achieved a balance between heat retention, vapour adsorption, and volumetric stability, attributed to the high porosity and specific surface area of the activated carbon. This material acted as a matrix of microcavities that absorbed thermal energy and regulated internal humidity, reducing the sensation of cold associated with environmental saturation.

Finally, the results showed that each additive offers distinct advantages: Ichu improves air retention and thermal resistance in controlled proportions, Linen stabilises the indoor microclimate with a better balance between density and conductivity, and activated carbon is the most efficient additive, combining thermal insulation with humidity regulation. This convergence of properties opens up the possibility of designing hybrid mixtures that integrate fibres

and activated carbon in balanced proportions, thus enhancing the performance of adobe roofs against frost. It is recommended to prioritise the use of activated carbon at 20% as a basis for intervention and to supplement it with fibres in optimal proportions (33% ichu and 60% Linen) in order to configure sustainable, replicable construction systems adapted to the rural Andean reality, with the capacity to mitigate the impact of extreme cold on the health and quality of life of vulnerable populations.

This strategy is also recommended for its replicability, as it can be implemented across different communities using local resources at low cost, thereby ensuring scalability and applicability in larger-scale rural housing programs. This assertion is based on the fact that the experiment was carried out under proportional geometric conditions and with materials representative of a real dwelling, which ensures the validity of the extrapolation.

## Additional Information

A link is attached to validate the instruments used by experts in the field.

Link:
https://drive.google.com/drive/folders/1NEsuqQOgKUPEJSKBjNMsPEUZVg36p6dq?usp=sharing

## Conflicts of Interest

We declare that there is no conflict of interest regarding the publication of this article.

## References


[1] Lourdes Gretel Pando Casabona, "*Design Proposal for A Reduced-Scale Two-Story Adobe House Model Reinforced with Rope Mesh*," Thesis, Pontifical Catholic University of Peru, Lima, Peru, 2021. [Google Scholar] [Publisher Link]

[2] National Institute of Statistics and Informatics, There are more than Ten Million Registered Private Homes in the Country, 2025. [Online]. Available: https://www.gob.pe/institucion/inei/noticias/535471-en-el-pais-existen-mas-de-diez-millones-de-viviendas-particulares-censadas

[3] D. Alejandro Arrieta, Social Determinants of Health Conditions in the Marginal Urban Population of Huancayo, Junín, pp. 311-330. [Online]. Available: https://www.desco.org.pe/recursos/site/files/CONTENIDO/1380/13_Arrieta_PHd20.pdf

[4] Jhon Edgar Zumaeta Delgado et al., Junín: Statistical Compendium, 2023. [Online]. Available: https://cdn.www.gob.pe/uploads/document/file/6203805/5468931-compendio-estadistico-junin-2023.pdf?v=1713298057

[5] Ridima Sharma, and Vandna Sharma, "Thermal Performance Study of Traditional Slate Roofed Mud Houses in the Sub-Tropical Sub Montane and Low Hills of Himachal Pradesh," *Visions for Sustainability*, no. 21, pp. 431-459, 2024. [CrossRef] [Google Scholar] [Publisher Link]

[6] Anthony Edgar Mamani Apaza, and Pedro Fernando Moran Ramirez, "*Evaluation of the Thermal Behavior of an Adobe with the Addition of Diatomite for the Construction of Houses in the Rural Areas of the Department of Ayacucho*," Thesis, Peruvian University of Applied Sciences (UPC), Lima, Peru, 2021. [Google Scholar] [Publisher Link]

[7] Jessica R. Molina et al., "High Andean Bioclimatic Dwellings in Peru: Climatic Conditions, Vulnerability of the Population and Review of Academic Studies and Massification Programmes," *Renewable and Sustainable Energy Reviews*, vol. 217, 2025. [CrossRef] [Google Scholar] [Publisher Link]

[8] Correo, Junín: 45 Deaths from Pneumonia and Warning of a Drop in Temperature, 2025. [Online]. Available: https://diariocorreo.pe/edicion/huancayo/junin-45-muertes-por-neumonia-y-alertan-descenso-de-temperatura-noticia/

[9] Fides News Agency Bolivia, South America Registers more than 170 Deaths Due to Winter, 23 in Bolivia, 2025. [Online]. Available: https://www.noticiasfides.com/nacional/sociedad/sudamerica-registra-mas-de-170-muertos-por-el-invierno-23-en-bolivia-269158

[10] Xinhua Español, Intense Winter Cold Causes 16 Deaths in Bolivian Department of La Paz, 2025. [Online]. Available: https://spanish.xinhuanet.com/20240725/4b842d51bb4f43c8bdc5aff59f641056/c.html

[11] Nepali Times, Nepalis Still Dying of Cold, 2021. [Online]. Available: https://nepalitimes.com/here-now/nepalis-still-dying-of-cold

[12] Alioska Jessica Martínez García et al., "Thermal Evaluation of a Rustic Building Prototype at 1/5 Scale with Vegetal Envelope During the Winter in Southern Peru," *Data and Metadata*, vol. 2, pp. 1-6, 2023. [CrossRef] [Google Scholar] [Publisher Link]

[13] Seda Nur Alkan, and Fatih Yazıcıoğlu, "Evaluation of the Hygrothermal Performance of Exterior Walls in Traditional Timber-Frame Residential Buildings: The Safranbolu and Zeyrek Example," *Gazi University Faculty of Engineering and Architecture Journal*, vol. 39, no. 2, pp. 1209-1222, 2024. [CrossRef] [Google Scholar] [Publisher Link]

[14] Enrique Mejia-Solis, Jaime Arias, and Björn Palm, "Simple Solutions for Improving Thermal Comfort in Huts in the Highlands of Peru," *Heliyon*, vol. 9, no. 10, pp. 1-14, 2023. [CrossRef] [Google Scholar] [Publisher Link]

[15] Flavio Roberto Ceja Soto et al., "Hydrothermal Evaluation of Vernacular Housing: Comparing Case Studies of Waste PET Bottles, Stone, and Adobe Houses," *Buildings*, vol. 12, no. 8, pp. 1-17, 2022. [CrossRef] [Google Scholar] [Publisher Link]

[16] Mohamed Lamrani et al., "Thermal Behaviour Assessment of a New Local Clay-based Building Material and Peanut Shell Waste: Experimental and Numerical Approaches," *Civil Engineering and Architecture*, vol. 11, no. 6, pp. 3451-3470, 2023. [CrossRef] [Google Scholar] [Publisher Link]

[17] Kusum Saini, Vasant A. Matsagar, and Venkatesh R. Kodur, "Recent Advances in the use of Natural Fibers in Civil Engineering Structures," *Construction and Building Materials*, vol. 411, 2024. [CrossRef] [Google Scholar] [Publisher Link]

[18] Chávez De la Cruz, and Raysa Milagros, "*Slope Stability Analysis in Sandstones using the Empirical Hazard Index, Kinematic and Limit Equilibrium Methods on the Tarapoto-Yurimaguas Road*," Thesis, Universidad Peruana De Ciencias Aplicadas, Lima, 2020. [CrossRef] [Google Scholar] [Publisher Link]

[19] Ichrak Hamrouni et al., "Thermal Properties of a Raw Earth-Flax Fibers Building Material," *Construction and Building Materials*, vol. 423, pp. 1-12, 2024. [CrossRef] [Google Scholar] [Publisher Link]

[20] Hyilda Jaci Dorregaray De La Cruz, "*Pineapple (Ananas Comosus) Fruit Peels to Remove Heavy Metals (Cd2+, Pb2+) from Aqueous Solutions*," Thesis, Universidad Nacional del Centro del Peru, Huancayo, 2018. [Google Scholar] [Publisher Link]

[21] Ruiz Cayetano et al., "*Organic Solid Waste Management in the Saño District-Huancayo Province 2021*," Thesis, National University of Central Peru, Huancayo, 2021. [Google Scholar] [Publisher Link]

[22] J.M. Pinas et al., "Influence of Stipa Ichu on the Thermal and Mechanical Properties of Adobe as a Biocomposite Material," *Journal of Physics: Conference Series*, vol. 1433, no. 1, pp. 1-11, 2020. [CrossRef] [Google Scholar] [Publisher Link]

[23] Felix Martin Gonzales Chea, "*Study of Ichu Fiber Incorporated as Thermal Insulation in a Dry Construction System for use in the Envelopes of Rural Houses Located in Cold Climatic Zones of Peru*," Thesis, Pontificia Universidad Católica del Perú, Lima, Peru, 2023. [Google Scholar] [Publisher Link]

[24] A. Guzman et al., "Thermal Conductivity of Insulating Materials using a Peltier Cell based Cooling System," *Journal of Physics: Conference Series*, vol. 2869, no. 1, pp. 1-7, 2024. [CrossRef] [Google Scholar] [Publisher Link]

[25] E. Palo-Tejada et al., "Low-Cost Portable System for Measuring Thermal Conductivity of Building," *Journal of Physics: Conference Series*, vol. 2180, no. 1, pp. 1-9, 2022. [CrossRef] [Google Scholar] [Publisher Link]

[26] Samuel Charca Mamani et al., "Assessment of Ichu Fibers as Non-Expensive Thermal Insulation System for the Andean Regions," *Energy and Buildings*, vol. 108, pp. 55-60, 2015. [CrossRef] [Google Scholar] [Publisher Link]

[27] Magdi El Messiry et al., "Development of High-Performance Thermal Insulation Panels from Flax Fiber Waste for Building Insulation," *Journal of Industrial Textiles*, vol. 55, pp. 1-32, 2025. [CrossRef] [Google Scholar] [Publisher Link]

[28] Valeria Cascione et al., "Evaluating Environmental Impacts of Bio-based Insulation Materials Through Scenario-based and Dynamic Life Cycle Assessment," *The International Journal of Life Cycle Assessment*, vol. 30, no. 4, pp. 601-620, 2025. [CrossRef] [Google Scholar] [Publisher Link]

[29] Rūta Stapulionienė et al., "Investigation of Thermal Conductivity of Natural Fibres Processed by Different Mechanical Methods," *International Journal of Precision Engineering and Manufacturing*, vol. 17, no. 10, pp. 1371-1381, 2016. [CrossRef] [Google Scholar] [Publisher Link]

[30] Sayed Waqar Azhar et al., "Fabrication and Mechanical Properties of Flaxseed Fiber Bundle-Reinforced Polybutylene Succinate Composites," *Journal of Industrial Textiles*, vol. 50, no. 1, pp. 98-113, 2020. [CrossRef] [Google Scholar] [Publisher Link]

[31] Pierre Ouagne et al., "Fibre Extraction from Oleaginous Flax for Technical Textile Applications: Influence of Pre-processing parameters on Fibre Extraction Yield, Size Distribution and Mechanical Properties," *Procedia Engineering*, vol. 200, pp. 213-220, 2017. [CrossRef] [Google Scholar] [Publisher Link]

[32] Monica Tonelli et al., "Activation of Ground Granulated Blast-Furnace Slag with Calcium Hydroxide Nanoparticles Towards the Consolidation of Adobe," *Construction and Building Materials*, vol. 439, pp. 1-12, 2024. [CrossRef] [Google Scholar] [Publisher Link]

[33] Donghui Seo, and Su-Gwang Jeong, "Dynamic Heat Transfer and Electric Energy Consumption Performance of Dry Floor Heating Systems Mixed with Low-Cost Phase-Change Material and Activated Carbon for Field Application," *Energy and Buildings*, vol. 337, 2025. [CrossRef] [Google Scholar] [Publisher Link]

[34] Ministry Sanitation, "Standard E.080 Design and Construction with Reinforced Earth," *Ministerial Resolution*, no. 121, 2017. [Google Scholar]

[35] Danilo Servando Carrasco Pacheco et al., "Influence of Rice Husk and Cabuya Fiber on the Physical and Mechanical Properties of Adobe," *Engineering and Applied Science Research*, vol. 52, no. 1, pp. 112-124, 2025. [CrossRef] [Google Scholar] [Publisher Link]

[36] Yonathan Muche Kasie, and Agegnehu Yihunie Mogne, "Improvement of Mechanical Properties of Adobe Brick Reinforced with Sisal Fiber," *Discover Materials*, vol. 5, no. 1, pp. 1-15, 2025. [CrossRef] [Google Scholar] [Publisher Link]

[37] Guillaume Polidori et al., "Analysis of Adobes from Vernacular Raw Earth Buildings in the Champagne Region (France)," *Construction and Building Materials*, vol. 470, pp. 1-14, 2025. [CrossRef] [Google Scholar] [Publisher Link]

[38] Nataly Cecilia Perez Curi et al., "Analysis of the Mechanical Properties of Adobe with Chillihua Fibre and Recycled LDPE for Sustainable Construction in the Andes," *Civil Engineering and Architecture*, vol. 13, no. 1, pp. 193-209, 2025. [CrossRef] [Google Scholar] [Publisher Link]

[39] Félix Jacinto Ccallo, Chambilla Maquera, and Wilber Andrés, "*Proposal for a Reinforced Adobe Housing Model with Earthquake-Resistant Metal Mesh for the Town of Lampa, District and Province of Lampa - Puno, Period 2020-2021*," Thesis, National University of the Altiplano, Puno, Peru, 2022. [Google Scholar] [Publisher Link]

[40] Roel Edison Mamani Condori, "*Prototype of Housing with Improved Adobe in the District of Chupa-Azángaro*," Thesis, National University of the Altiplano, Puno, Peru, 2017. [Google Scholar] [Publisher Link]

[41] Myriam Alexandra Torres Paucar, "*Prototype of an Emergency Modular Housing Unit, made with Stabilized Adobe, for the Event of an Eruption of the Cotopaxi Volcano*," Thesis, University of Extremadura, Plasencia, Spain, 2017. [Google Scholar] [Publisher Link]

[42] E. Leroy Torres, "Getty Seismic Adobe Project Research and Testing Program," *Proceedings of Getty Seismic Adobe Project 2006 Colloquium*, Los Angeles, California: The Getty Conservation Institute, pp. 34-41, 2009. [Google Scholar]

[43] Josafat Silvestre Prada Sulca, Nelson Gustavo Huillca Lopez, and Carlos Augusto Eyzaguirre Acosta, "*Adobe House Design with Totora Mat Cladding to Improve Thermal Comfort in the Ayacucho District of the Huamanga Province in the Ayacucho Department*," Thesis, Peruvian University of Applied Sciences (UPC), Lima, Peru, 2023. [Google Scholar] [Publisher Link]

[44] Roger L. Shannon, "Thermal Scale Modeling of Radiation-Conduction-Convection Systems," *Journal of Spacecraft and Rockets*, vol. 10, no. 8, pp. 485-492, 1973. [CrossRef] [Google Scholar] [Publisher Link]

[45] E. Zapana Quispe, "Materials for the Construction of a Sustainable House in the Peruvian Highlands," *Taypi Architecture and Urbanism Magazine*, vol. 1, no. 3, pp. 15-22, 2023. [CrossRef] [Google Scholar] [Publisher Link]

[46] Manuel Martin-Brañas, and Albert Iman-Torres, "Thermal Analysis of two Types of Roof used in Rural Amazonian Houses," *Amazonian Folia*, vol. 23, no. 2, pp. 105-118, 2014. [CrossRef] [Google Scholar] [Publisher Link]

[47] MCA, Metal Roof Design for Cold Climates. [Online]. Available: https://www.metalconstruction.org/index.php/online-education/Metal-Roof-Design-for-Cold-Climates

[48] Miguel Angel Alban Alcívar, Jorge Lider Macias Ramos, and Danny Emir Alcivar Velez, "Influence of the Orientation and the Angle of Inclination in the Metal Roof," *Linguistics and Culture Review*, vol. 6, no. on, pp. 140-157, 2022. [CrossRef] [Google Scholar] [Publisher Link]

[49] Domenico Mazzeo, and Karolos J. Kontoleon, "The role of Inclination and Orientation of Different Building Roof Typologies on Indoor and Outdoor Environment Thermal Comfort in Italy and Greece," *Sustainable Cities and Society*, vol. 60, 2020. [CrossRef] [Google Scholar] [Publisher Link]

[50] Yichen Han et al., "Enhancing Building Energy Efficiency with Thermal Mass Optimization," *Advances in Applied Energy*, vol. 18, pp. 1-15, 2025. [CrossRef] [Google Scholar] [Publisher Link]

[51] Qudama Al-Yasiri, Mohammed Alktranee, and Márta Szabó, "Metal Fibers-Enhanced PCM Thermal Energy Storage Unit: An Experimental Approach on a Composite Roof Application," *International Journal of Thermofluids*, vol. 23, pp. 1-9, 2024. [CrossRef] [Google Scholar] [Publisher Link]

[52] Samira Noohi, and Davood Rezaei, "Operation of Roof Pond Systems, Considering its Advantages and Disadvantages," *Conference: The 6. International Green Energy Conference IGEC-6*, Eskisehir (Turkey), pp. 5-9, 2011. [Google Scholar] [Publisher Link]

[53] Vladimir Montoya Torres, and Jhomara Rojas Tacza, "Bio Thermal Panels Applied to the Comfort of Rural Homes in the District of Sincos in 2024," *E3S Web of Conferences*, vol. 620, pp. 1-12, 2025. [CrossRef] [Google Scholar] [Publisher Link]

[54] Luis Felipe Godoy Vaca et al., "Energy Analysis of Adobe Performance as a Housing Construction Material in Ecuador," *International Journal of Mathematics in Operational Research*, vol. 18, no. 2, pp. 154-168, 2021. [CrossRef] [Google Scholar] [Publisher Link]

[55] S. Charca, and S. Candiotti, "Mechanical Properties Characterization of the Ichu Fibers Composites," *IOP Conference Series: Materials Science and Engineering*, vol. 942, no. 1, pp. 1-8, 2020. [CrossRef] [Google Scholar] [Publisher Link]

[56] Sandra Mori et al., "Physical and Thermal Properties of Novel Native Andean Natural Fibers," *Journal of Natural Fibers*, vol. 18, no. 4, pp. 475-491, 2021. [CrossRef] [Google Scholar] [Publisher Link]

[57] Gaby Maribel Atahuachi Layme, and Yanet Nayda Carcausto Quispesayhua, "*Thermoacoustic Insulation based on STIPA Ichu to Reduce Noise and Drastic Temperature Changes in Homes in Urban Expansion Areas of the City of Puno*," Thesis, National University of the Altiplano, Puno, Peru, 2018. [Google Scholar] [Publisher Link]

[58] Virginia Astocuri Ríos, "*Potential of Natural Resources for Livestock Farming in the Communal Territory of Saño-Huancayo-Junín*," Thesis, National University of Central Peru, Huancayo, Perú, 2015. [Google Scholar] [Publisher Link]

[59] Senamhi, Weather Forecast for Huancayo (Junín), Weather / Weather Forecast. [Online]. Available: https://www.senamhi.gob.pe/main.php?dp=junin&p=pronostico-detalle

[60] Alberto Lopez-Arraiza et al., "Life Cycle Assessment of Glass Fibre Versus Flax Fibre Reinforced Composite Ship Hulls," *Scientific Reports*, vol. 15, no. 1, pp. 1-12, 2025. [CrossRef] [Google Scholar] [Publisher Link]

[61] Awoke Fenta Wodag et al., "Enhancing Mechanical and Thermal Properties of Three Dimensional (3D) Woven Flax Fiber/ Polylactic Acid (PLA) Green Composites," *Materials Today Communications*, vol. 46, 2025. [CrossRef] [Google Scholar] [Publisher Link]

[62] Paolino Cassese et al., "In-Plane Shear Behaviour of Adobe Masonry Wallets Strengthened with Textile Reinforced Mortar," *Construction and Building Materials*, vol. 306, pp. 1-33, 2021. [CrossRef] [Google Scholar] [Publisher Link]

[63] Franco Mauricio et al., "Scientometric Analysis of Activated Carbon or Probiotics in Mouthwashes or Toothpastes: Dynamicity, Spatiotemporal Evolution and Trends," *ODOVTOS - International Journal of Dental Sciences*, vol. 27, no. 1, pp. 52-63, 2025. [CrossRef] [Google Scholar] [Publisher Link]

[64] Yanqin Chen et al., "Enhanced Adsorption of Phenol using EDTA-4Na- and KOH-Modified Almond Shell Biochar," *Sustainable Environment Research*, vol. 35, no. 1, pp. 1-18, 2025. [CrossRef] [Google Scholar] [Publisher Link]

[65] Eric Jhon Cruz, John Julius Manuben, and Maria Lorena Cruz, "Removal of Pesticide Residues in Aqueous Solution by Adsorption using Pineapple Peel Activated Carbon," *Journal of Environmental Science and Management*, no. 1, pp. 47-56, 2023. [CrossRef] [Google Scholar] [Publisher Link]

[66] S.N. Turkmen Koc et al., "Removal of Zinc from Wastewater using Orange, Pineapple and Pomegranate Peels," *International Journal of Environmental Science and Technology*, vol. 18, no. 9, pp. 2781-2792, 2020. [CrossRef] [Google Scholar] [Publisher Link]

[67] N.F. Abd Ghapar, R. Abu Samah, and S. Abd Rahman, "Pineapple Peel Waste Adsorbent for Adsorption of Fe (III)," *IOP Conference Series: Materials Science and Engineering*, vol. 991, no. 1, pp. 1-5, 2020. [CrossRef] [Google Scholar] [Publisher Link]

[68] Chun On Chin et al., "Mechanical and Thermal Properties of Lightweight Concrete Incorporated with Activated Carbon as Coarse Aggregate," *Journal of Building Engineering*, vol. 31, 2020. [CrossRef] [Google Scholar] [Publisher Link]

[69] Vladimir Simon Montoya Torres, and Aida Diana Baltazar Ramos, "Use of Biopanels in Bagasse-Derived Ceilings for Thermal Comfort in Homes in the Sierra - Altoandina, Aramachay, Jauja," *Civil Engineering and Architecture*, vol. 13, no. 2, pp. 1305-1316, 2025. [CrossRef] [Google Scholar] [Publisher Link]

[70] Ciro Abelardo Espinoza Montes, "*Solar Heating System to Reduce the Cold in High Andean Homes*," Thesis, National University of Central Peru, Huancayo, Peru, 2013. [Google Scholar] [Publisher Link]

[71] Senamhi, Frost and Cold Waves / Frequently Asked Questions, Climate / Frost and Cold Spells. [Online]. Available: https://www.senamhi.gob.pe/main.php?dp=junin&p=heladas-y-friajes-preguntas

[72] Peruvian News Agency Andina, Minimum Temperature in Huancayo Reached 6.2 Degrees Below Zero, 2025. [Online]. Available: https://andina.pe/agencia/noticia-temperatura-minima-huancayo-llego-a-62-grados-bajo-cero-421663.aspx

[73] Cevdet Emin Ekinci, and Belkis Elyigit, "The Effect of the Aggregate Size and Ambient Temperature on the Impact Resistance of Concrete," *International Journal of Concrete Structures and Materials*, vol. 19, no. 1, pp. 1-19, 2025. [CrossRef] [Google Scholar] [Publisher Link]

[74] J. Vijayalaxmi, and Dhananjay Hete, *An Analytical Assessment and Retrofit using Nanomaterials of Rural Houses in Heat Wave-Prone Region in India*, Building Thermal Performance and Sustainability, Springer, Singapore, vol. 316, pp. 177-191, 2023. [CrossRef] [Google Scholar] [Publisher Link]

[75] Andreia Furtado et al., "Frost/Dew Point Temperature and Relative Humidity Measurements: Primary and Secondary Calibration Methods," *EPJ Web Conference*, vol. 323, pp. 1-6, 2025. [CrossRef] [Google Scholar] [Publisher Link]

[76] Cristiano Zanetti, "Made in the Galleries of His Most Serene Highness, Florence'. Conflicts in Instrument Invention at the Medici Court: The Pendulum Clock, and the Accademia Del Cimento," *Annals of Science*, vol. 83, no. 2, pp. 279-325, 2026. [CrossRef] [Google Scholar] [Publisher Link]

[77] Taichi Shirasawa et al., "Proposal of Wind Force Scale based on Wind Speed Measurement and Free-Text Description by Local Residents," *Journal of Environmental Engineering (Japan)*, vol. 89, no. 825, pp. 694-701, 2024. [CrossRef] [Google Scholar] [Publisher Link]

[78] Shaifali M. Arora, and Mishti Gautam, *Automated Weather Monitoring Station based on IoT for Smart Cities*, IoT for Sustainable Smart Cities and Society, Springer, Cham, pp. 227-243, 2022. [CrossRef] [Google Scholar] [Publisher Link]

[79] Laura Carnieletto et al., "Italian Prototype Building Models for Urban Scale Building Performance Simulation," *Building and Environment*, vol. 192, pp. 1-32, 2021. [CrossRef] [Google Scholar] [Publisher Link]

[80] Alessandro Casaburo et al., "A Review of Similitude Methods for Structural Engineering," *Applied Mechanics Reviews*, vol. 71, no. 3, pp. 1-32, 2019. [CrossRef] [Google Scholar] [Publisher Link]

[81] Juan M. Lirola et al., "A Review on Experimental Research using Scale Models for Buildings: Application and Methodologies," *Energy and Buildings*, vol. 142, pp. 72-110, 2017. [CrossRef] [Google Scholar] [Publisher Link]

[82] Gabo Cyprien Bailly et al., "Advancing Earth-based Construction: A Comprehensive Review of Stabilization and Reinforcement Techniques for Adobe and Compressed Earth Blocks," *Eng*, vol. 5, no. 2, pp. 750-783, 2024. [CrossRef] [Google Scholar] [Publisher Link]

[83] G. Araya-Letelier et al., "Influence of Natural Fiber Dosage and Length on Adobe Mixes Damage-Mechanical Behavior," *Construction and Building Materials*, vol. 174, pp. 645-655, 2018. [CrossRef] [Google Scholar] [Publisher Link]

[84] Weinan Han et al., "Compressive Performance of Adobe Masonry Strengthened with Glass-Fiber Reinforced Matrix Composites," *Materials and Structures*, vol. 56, no. 3, 2023. [CrossRef] [Google Scholar] [Publisher Link]